

TESTING THE RENAL SIGNALING AXIS FOR FGF23

Pu Ni

Submitted to the faculty of the University Graduate School

in partial fulfillment of the requirements

for the degree

Master of Science

in the Department of Medical and Molecular Genetics,

Indian University

December 2015

Accepted by the Graduate Faculty, Indiana University, in partial fulfillment of the requirements for the degree of Master of Science.

Master's Thesis Committee

Kenneth E. White, Ph.D., Chair

Brittney-Shea Herbert, Ph.D.

Stephen Dlouhy, Ph.D.

ACKNOWLEDGEMENT

I would like to express my gratitude first to my mentor, Dr. Kenneth E. White for giving me this opportunity to start my research experience in the laboratory. Thanks for his great patience, understanding and motivation. With his guidance, I am able to complete my graduate research and thesis writing successfully and confidently. I am very fortunate to join his laboratory and benefit from his wide knowledge.

I would like to thank my other committee members, Dr. Brittney-Shea Herbert and Dr. Stephen Dlouhy for their constant encouragement and their suggestions within my research progress.

I also want to thank my labmates, Dr. Erica Clinkenbeard, Dr. Julia M. Hum, Dr. Hitesh Nidumanda Appaiah and Taryn Audrey Cass. Especially for Dr. Erica Clinkenbeard, I am grateful to her patient instructions and great time devoting to training me, helping me become a better researcher.

Last but not the least, I thank my family for supporting my study abroad economically and spiritually. Thanks to my friends in Indianapolis, especially my roommate Ruchi Bansal for being here with me all the time and helping me out with my thesis formatting and language usage, also for her continuous encouragement.

TESTING THE RENAL SIGNALING AXIS FOR FGF23

FGF23 is the central regulator for phosphate homeostasis. Both FGF23 and phosphate dysregulation are highly related with the progression of chronic kidney disease (CKD), which is a global health problem. In previous studies, FGF23 was found to be produced in bone and targeting the kidneys to regulate phosphate reabsorption and excretion. In the FGF23 signaling axis, it binds a receptor complex (α Klotho and FGFRs) in the distal convoluted tubules (DCT) and causes its biological effects in the proximal tubules (PT). The mechanism of how the signals passing on from DCT to PT is not clear.

In my research, experiments were focused on the FGF23 signaling pathway within the kidney to study the communication steps between tubular cells. HBEGF treatment was given to FGF23 signaling impaired mouse models resulting in significant change of genes regulated by FGF23, indicating that HBEGF was important in the FGF23 signaling axis. Then high quality rabbit anti-mouse HBEGF antibodies were made to better study HBEGF activity *in vivo* and *in vitro*. A new cell model was characterized to test FGF23 effects on HBEGF signaling using Western blots and immunofluorescence. Lastly, the location of HBEGF activity was examined in the kidney *in vivo*. Immunostaining suggested that HBEGF activated the mitogen activated protein kinase (MAPK) pathway. This mapping may provide important information for the molecular relationships between FGF23 and HBEGF.

Kenneth E. White, Ph.D., Chair

TABLE OF CONTENTS

| | |
|---|------|
| List of Tables | viii |
| List of Figures | ix |
| List of Abbreviations | x |
| Introduction..... | 1 |
| Phosphate Regulation..... | 1 |
| General introduction to the control of phosphate | 1 |
| Hormonal regulation in specialized organs..... | 2 |
| FGF23 | 5 |
| FGF23 general characteristics..... | 5 |
| FGF23 biological activities and regulation..... | 6 |
| FGF23 receptor complex | 7 |
| FGF23 animal models..... | 11 |
| Disorders involving phosphate metabolism..... | 12 |
| Autosomal Dominant Hypophosphatemic Rickets (ADHR)..... | 12 |
| X-Linked Hypophosphatemic Rickets (XLH)..... | 13 |
| Autosomal Recessive Hypophosphatemic Rickets (ARHR)..... | 14 |
| Hyperphosphatemic Familial Tumoral Calcinosis (hFTC)..... | 15 |
| Chronic Kidney Disease (CKD) | 16 |
| Hypothesized molecular pathway for FGF23 activity in kidney | 19 |
| Gene expression changes after FGF23 administration | 19 |
| Hypothesis for HBEGF participation in FGF23 signaling | 19 |
| General properties of HBEGF | 22 |

| | |
|---|----|
| HBEGF processing and signaling..... | 22 |
| Global Hypothesis..... | 25 |
| Materials and Methods..... | 27 |
| Animal Studies..... | 27 |
| Cell Culture..... | 28 |
| Immunoblotting..... | 29 |
| Immunofluorescence..... | 31 |
| Quantitative PCR..... | 34 |
| HBEGF antibody..... | 36 |
| Other materials..... | 37 |
| Statistical Analysis..... | 37 |
| Results..... | 38 |
| Initial study of HBEGF activity <i>in vivo</i> | 38 |
| Preparation of an HBEGF antibody..... | 43 |
| <i>In vitro</i> model for HBEGF characterization..... | 49 |
| HBEGF signal mapping <i>in vivo</i> | 54 |
| Discussion..... | 59 |
| Thesis summary..... | 59 |
| <i>In vivo</i> study analysis..... | 60 |
| Identifying involved gene changes in FGF23 signaling..... | 60 |
| Gene expression changes in FGF23-related knockout mouse models..... | 61 |
| HBEGF pathway immunofluorescence in kidney sections..... | 63 |
| <i>In vitro</i> study analysis..... | 64 |

| | |
|---|----|
| A cell model being tested..... | 64 |
| <i>In vitro</i> study optimization..... | 65 |
| Alternative hypothesis to FGF23 signaling | 67 |
| Conclusion | 69 |
| References..... | 72 |
| Curriculum Vitae | |

List of Tables

| | |
|---|----|
| Table 1 Primary inherited phosphate disorders involving FGF23 | 18 |
| Table 2 Kidney microarray data after acute FGF23 administration | 21 |
| Table 3 Primary antibodies for WB | 30 |
| Table 4 Secondary antibodies for WB | 31 |
| Table 5 Primary antibodies for IF | 32 |
| Table 6 Secondary antibodies for IF | 32 |
| Table 7 Real-time PCR Primers..... | 35 |
| Table 8 Recombinant Protein..... | 37 |
| Table 9 Other Chemicals | 37 |

List of Figures

| | |
|--|----|
| Figure 1 Phosphate homeostasis | 4 |
| Figure 2 Hormonal regulation of FGF23 | 8 |
| Figure 3 FGF23 renal signaling pathways and bioactivity mapping | 10 |
| Figure 4 Structure and processing of HBEGF | 24 |
| Figure 5 FGF23 hypothesized downstream signaling | 26 |
| Figure 6 q-PCR analysis of HBEGF administration in α KL-KO mice | 40 |
| Figure 7 q-PCR analysis of HBEGF administration to FGF23-KO mice | 42 |
| Figure 8 HBEGF structure and immune polypeptide | 44 |
| Figure 9 HBEGF antibody characterization | 45 |
| Figure 10 <i>In vitro</i> HBEGF antibody testing | 48 |
| Figure 11 Hypothesized HBEGF signaling <i>in vitro</i> | 50 |
| Figure 12 Potential cell model characterization..... | 53 |
| Figure 13 P-Erk staining mapping <i>in vivo</i> (1)..... | 55 |
| Figure 14 P-Erk staining mapping <i>in vivo</i> (2)..... | 58 |
| Figure 15 α KL mapping in the kidneys | 68 |
| Figure 16 Alternative hypothesized pathway for renal FGF23 signaling..... | 71 |

List of Abbreviations

| | |
|----------|--|
| ADHR | Autosomal dominant hypophosphatemic rickets |
| ARHR | Autosomal recessive hypophosphatemic rickets |
| BBM | Brush-border membrane |
| CAS | CRISPR-associate endonuclease |
| CKD | Chronic kidney disease |
| CRISPR | Clustered regularly interspaced short palindromic repeat |
| DCT | Distal convoluted tubule |
| DMP1 | Dentin matrix protein 1 |
| DOX | Doxycycline |
| EGF | Epidermal growth factor |
| EGR1 | Early growth response protein 1 |
| ELISA | Enzyme linked immunosorbent assay |
| ENPP1 | Ectonucleotide pyrophosphatase/phosphodiesterase-1 |
| ERK | Extracellular signal-regulated kinase |
| FAM20c | Family with sequence similarity 20, member c |
| FGF23 | Fibroblast growth factor 23 |
| GALNT3 | Polypeptide N-acetylgalactosaminyl transferase-3 |
| GFR | Glomerular filtration rate |
| HBEGF/HB | Heparin binding EGF-like growth factor |
| HEK293 | Human embryonic kidney 293 cell line |
| hFTC | Hyperphosphatemic Familial Tumoral calcinosis |
| IRH | Isolated recessive renal hypomagnesemia |

| | |
|--------------------------------------|---|
| i.v. | Intravenous |
| i.p. | Intraperitoneal |
| KL | Klotho |
| KO | Knock out |
| LTL | Fluorescein labeled lotus tetragonolobus lectin |
| MAPK | Mitogen activated protein kinase |
| NGS | Next generation sequencing |
| NPT2 | Type II sodium phosphate co-transporter |
| Pi | Phosphate |
| PHEX | Phosphate-regulating gene with homologies to endopeptidases on the X chromosome |
| PT | Proximal tubule |
| PTH | Parathyroid hormone |
| P-Erk1/2 | Phospho-Erk1/2 |
| P-EGFR | Phospho-epidermal growth factor receptor |
| ROS | Reactive oxygen species |
| rtTA | Reverse tetracycline-controlled transactivator |
| SPC | Subtilisin-like proprotein convertase |
| TPA | Phorbol 12-myristate 13-acetate |
| TRE | Tetracycline-response element |
| WT | Wild type |
| XLH | X-linked hypophosphatemia |
| 1,25(OH) ₂ D ₃ | 1,25-dihydroxyvitamin D ₃ |

| | |
|--------------------------|---|
| 1 α (OH)ase | 25-hydroxyvitamin D 1- α hydroxylase |
| 24(OH)ase | 1,25-dihydroxyvitamin D ₃ 24 hydroxylase |
| β -mercaptoethanol | β -ME |

Introduction

Phosphate Regulation

General introduction to the control of phosphate

Phosphate accounts for approximately one percent of a human's body weight. About eighty five percent is stored in bones as inorganic phosphate, whereas the rest resides in non-osseous tissues and the extracellular fluid. Phosphate is essential for a number of processes, including bone mineralization, cellular membrane formation, intracellular signaling and energy storage. The normal plasma phosphate range in adults is 2.5-4.5 mg/dl and in children is 4.0-6.5 mg/dl [1]. Plasma phosphate concentrations are determined by a balance of interactions among bone, small intestine and kidney (Figure 1). The main organ for phosphate storage is bone, in which phosphate gets mineralized with calcium as hydroxyapatite. Phosphate is abundant in a normal person's dietary intake so that most individuals get sufficient phosphate through small intestinal absorption [2]. After being absorbed into the circulation, proper phosphate levels are required for its biological activities. To keep phosphate in the normal physiological range, the kidney functions as a secretory organ. After phosphate gets filtered in glomeruli, specific renal tubules reabsorb the proper amount of phosphate for maintaining homeostasis. This regulation is important for major diseases, such as chronic kidney diseases (CKD), where phosphate homeostasis is disturbed (see below).

Hormonal regulation in specialized organs

The absorption rate of phosphate in the small intestine is primarily dependent on dietary intake, and is also influenced by the hormonal factor 1,25-dihydroxyvitamin D₃ (1,25-(OH)₂D₃). Vitamin D 1 α (OH)ase is a mitochondrial enzyme, which is expressed in the renal proximal tubule (PT) and converts inactive vitamin D to its active form 1,25-(OH)₂D₃. 1,25-dihydroxyvitamin D₃ 24 hydroxylase (24(OH)ase) is the enzyme that degrades 1,25-(OH)₂D₃. There are two primary mechanisms in the small intestine for phosphate absorption: one method is mediated by an active transporter, the sodium dependent co-transporter NPT2b, and the other occurs through paracellular trans-membrane diffusion, which is sodium independent. Active vitamin D works on the sodium dependent active transport mechanism to increase phosphate and calcium absorption [3]. Low blood phosphate levels are important factors to initiate active vitamin D synthesis, and 1,25-(OH)₂D₃ negatively regulates its formation through increasing the expression of the 24(OH)ase.

The kidneys are the critical organ for maintaining minute to minute serum phosphate levels through balancing reabsorption and secretion. The type II sodium phosphate co-transporters NPT2a and NPT2c, members of the sodium-phosphate co-transporter family, primarily control phosphate reabsorption. These transporters are located on the brush-border membrane (BBM) of proximal tubular cells [4]. Sodium-phosphate co-transporters actively transport phosphate from the tubule lumen of proximal tubular cells. Then phosphate is passed on to the bloodstream. The expression of the NPTs is regulated by

various factors, including dietary phosphate uptake, parathyroid hormone (PTH) [4], and FGF23 [5]. In mice, NPT2a influences phosphate transport greater than NPT2c [4], whereas NPT2c may play a larger role in humans. These co-transporters get internalized and degraded when PTH [6], FGF23 and serum phosphate are high, thus leading to reduced phosphate reabsorption.

Parathyroid hormone (PTH) also plays an important role in $1,25\text{-(OH)}_2\text{D}_3$ regulation and phosphate excretion. PTH initiates its activity through binding with PTH receptors in specific tissues and activates its G-protein coupled receptor, leading to intracellular signaling [7]. The principal function of PTH is to regulate calcium concentrations. When serum calcium is low, PTH mobilizes bone turnover to release calcium from bone reservoirs and increases $1\alpha\text{(OH)ase}$ expression to produce more active vitamin D, which helps to increase calcium absorption in the small intestine and retain calcium from being excreted by the kidneys. However, bone turnover can result in a simultaneous increase in phosphate, which has negative effects on the regulation of calcium. Thus PTH works on kidney tubules to enhance phosphate excretion [8], and in general, PTH regulates phosphate as a secondary action compared with calcium regulation. As hormonal factors target bone, PTH and $1,25\text{-(OH)}_2\text{D}_3$ act synergistically to facilitate moving phosphate into the blood to keep phosphate levels within the normal range.

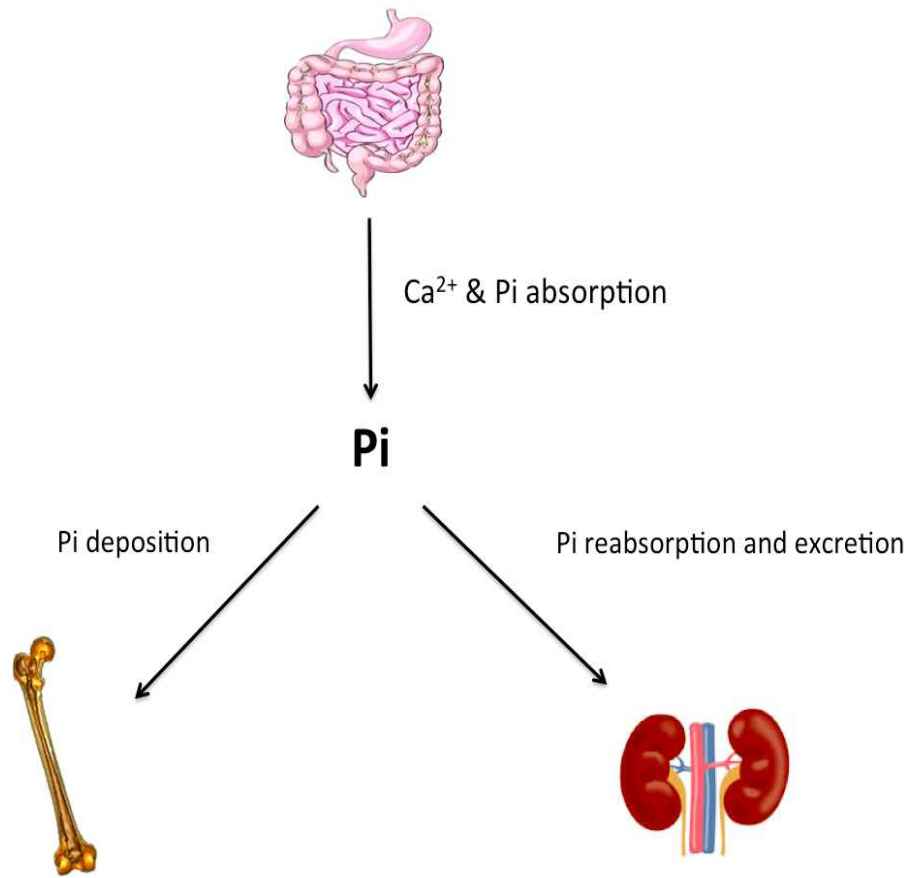


Figure 1 Phosphate homeostasis

In normal individuals, phosphate is absorbed from the diet in the small intestine. After entering the blood, circulating phosphate is filtered in the kidneys, in which the appropriate amount is reabsorbed for phosphate (Pi) balance. Bone is the reservoir for long-term phosphate storage.

FGF23

FGF23 general characteristics

Fibroblast growth factor 23 (FGF23) is a member of the human-mouse fibroblast growth factor gene family. Human FGF19 gene is the ortholog of mouse FGF15, thus the FGF family has 22 members in total [9]. FGF23 was first identified in the year 2000 as the gene for Autosomal Dominant Hypophosphatemic Rickets (ADHR, see below), a Mendelian disorder of disturbed phosphate metabolism. In this study, investigators combined gene information from four ADHR pedigrees using linkage analysis to identify FGF23 and its missense mutations in ADHR [10].

The FGF23 gene localizes on chromosome 12p13.13 and contains three exons which span 11,502 bases of genomic sequence. The gene encodes the 251 amino acids protein, whose full length is 32kD, which can be cleaved into fragments of 20kD and 12kD [11]. FGF23 is mainly produced in osteocytes and osteoblasts [12] and has low expression in the heart, liver and thyroid/parathyroid [10]. The full length FGF23 is the biologically active form [11]. Once cut into two fragments, FGF23 becomes inactive. The cleavage site is a R₁₇₆XXR₁₇₉ motif, and in the study of ADHR, FGF23 missense mutations of R176Q, R179Q and R179W were found to be the cause of impaired phosphate regulation [10]. Mutated FGF23 is resistant to endopeptidase cutting, which stabilizes active FGF23 and leads to phosphate wasting [11].

FGF23 biological activities and regulation

Although FGF23 is predominantly produced in bone, it targets the kidney to regulate phosphate and vitamin D metabolism. For direct phosphate regulation, FGF23 initiates NPT2a and NPT2c protein internalization and subsequent degradation, leading to phosphate wasting. *In vivo* models have supported these events. When wild type mice were injected with recombinant FGF23, serum phosphate levels decreased significantly compared with vehicle injections within 12 hours and NPT2a was down-regulated [5]. Mice with FGF23 delivery also showed a rapid, significantly reduced $1\alpha(\text{OH})\text{ase}$ expression and up-regulated $24(\text{OH})\text{ase}$ transcription, resulting in decreasing active vitamin D, before serum phosphate changes [13]. In a FGF23-overexpressing transgenic mouse model, NPT2a protein levels and mRNA expression were significantly decreased compared with wild type mice, and $1,25(\text{OH})_2\text{D}_3$ was significantly reduced [14]. A mouse model for X-linked hypophosphatemia (XLH), the Hyp mice showed elevated serum FGF23 concentrations, leading to reduction of NPT2a in proximal tubules [15]. In normal mice, low concentrations of blood phosphate triggers production of active vitamin D for phosphate absorption in the small intestine. However, with FGF23 administration, although there are low phosphate levels, active vitamin D is not produced. Thus, FGF23 down-regulates not only phosphate but also vitamin D formation in the kidneys.

As FGF23 has central effects on phosphate and vitamin D serum concentrations, their metabolites are also believed to participate in FGF23 regulation. Both in humans and animal models, phosphate supplements and depletion cause FGF23 increases and

decreases, respectively [16] [17]. In mouse models, 1,25(OH)₂D₃ injections led to dose-dependent increases of serum FGF23 levels, which was prior to phosphate concentration changes [13], suggesting that active vitamin D may regulate FGF23 directly through its promoter (see Figure 2).

FGF23 receptor complex

FGFRs: There are four FGF receptors (FGFRs) to mediate FGF bioactivity. FGFR1-FGFR4 are composed of an extracellular region containing a ligand binding domain and a heparin binding domain, a transmembrane region and an intracellular tyrosine kinase region. The FGFs bind to FGFRs, causing phosphorylation of the receptors and transmitting their biological functions [18]. Due to alternative splicing, each FGFR has various isoforms that have their own tissue specificities and biological activations. FGF23 has weak affinity to the FGFRs, suggesting it might require co-receptors to perform its bioactivities [19]. Indeed, investigators found that alpha-Klotho (α KL) knockout mice and FGF23 knockout mice shared common phenotypes, such as growth retardation, short life span, hyperphosphatemia and ectopic calcification, indicating α KL and FGF23 might have common signaling pathways. It was then proven *in vitro* that α KL is the co-receptor for FGF23 by co-expressing these proteins [20].

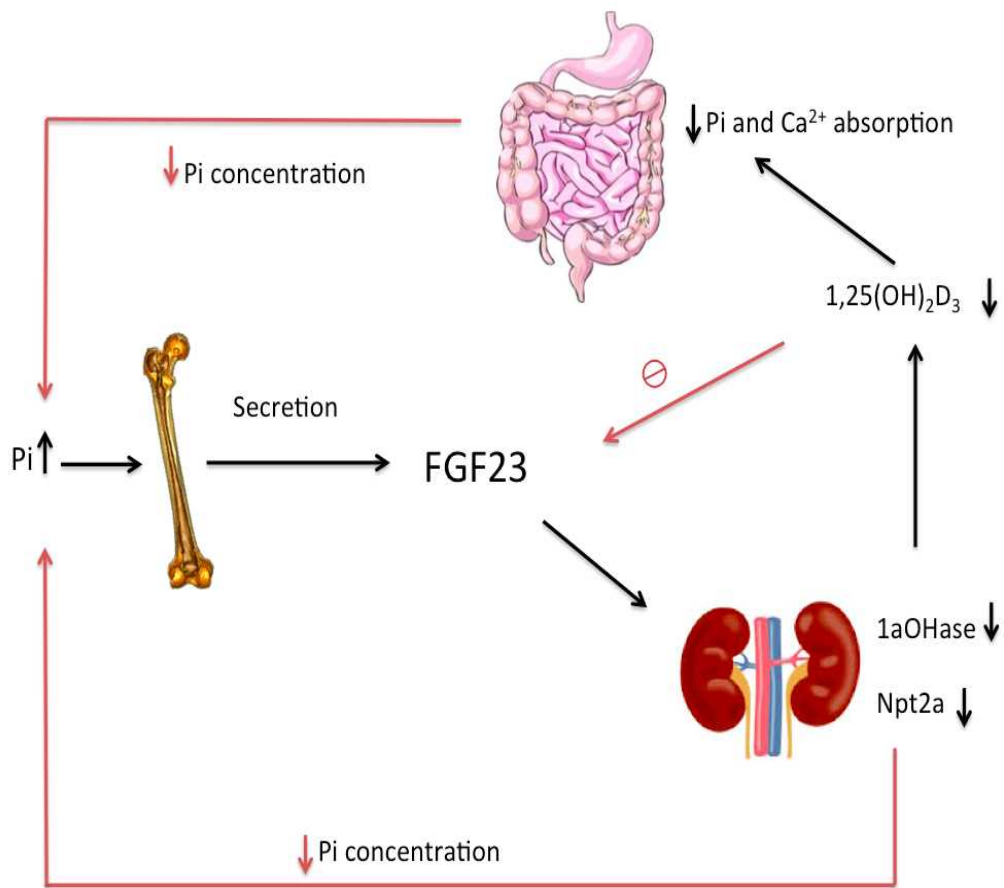


Figure 2 Hormonal regulation of FGF23

FGF23 is predominantly expressed in bone and secreted as a humoral factor to act on the renal proximal tubules in kidneys. It decreases proximal tubule 1 α (OH)ase expression, resulting in decreased active vitamin D and internalized NPT2a to reduce phosphate levels.

Alpha-Klotho: α KL was first hypothesized to be an aging gene, as the α KL deficient mouse model manifested early death as well as potential aging phenotypes. In humans, the α KL gene locates on chromosome 13q12, spans approximately 50Kbp and contains 5 exons, whereas in mice it is on chromosome 5. The α KL protein has two different isoforms due to protease activity. The first isoform is full length α KL, which is a membrane bound form (mKL), 130kD in size, containing a large extracellular domain and a very short (11 residues) intracellular region that is not sufficient for cytoplasmic signaling [21]. mKL can be cut near the membrane surface to produce a circulating form (cKL) that has a molecular mass of about 65kD. This cKL form is believed to work as a hormonal factor in multiple organs [22].

As the co-receptor for FGF23, α KL binding with FGFR leads to a 10-fold higher affinity for FGF23 than FGFRs alone [20]. FGF and FGFRs commonly activate the mitogen activated protein kinase (MAPK) pathway, and in kind FGF23 initiates the MAPK pathway and downstream phosphorylation. In the kidneys, α KL is localized in distal convoluted tubules (DCT). In a mouse study with 10-min tail vein injections of FGF23, phospho-ERK1/2 (P-Erk1/2) signaling, part of the MAPK pathway, was observed in DCT [23]. This suggests that FGF23 acts on the DCT through α KL-FGFR complexes. However, FGF23 regulates NPT2 and 1α (OH)ase in the PT, thus the mechanism of how FGF23 signals are delivered from DCT to PT is unknown (Figure 3).

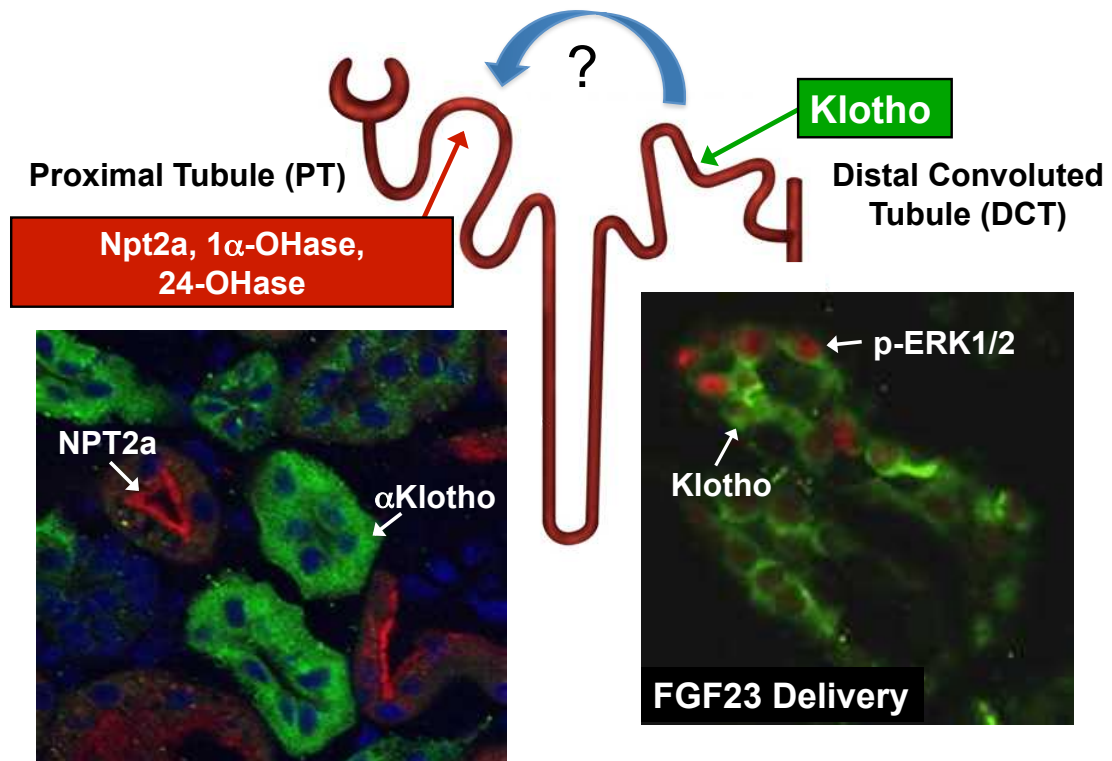


Figure 3 FGF23 renal signaling pathways and bioactivity mapping

In mice, (left) co-staining for Npt2a (red) and KL (green) proves separate locations of these two proteins in the renal tubule (left panel). After acute FGF23 delivery (right panel), the kidney was co-stained with anti-P-Erk1/2 (red) and anti-KL (green), and their signals overlapped; thus FGF23 signaling is separate from FGF23 function.

[Figure courtesy: Dr. Emily Farrow and Dr. Kenneth White]

FGF23 animal models

As FGF23 plays an essential role in phosphate handling through controlling phosphate reabsorption in the kidneys, animal models with FGF23 signaling insufficiency have been useful tools for testing the mechanisms underlying its bioactivity.

To better understand the role of FGF23 in phosphate homeostasis, FGF23 knockout (KO) mice and transgenic mice overexpressing FGF23 were developed. In one FGF23-KO mouse model developed by our laboratory, exon 2 of the FGF23 gene is deleted globally using the Cre-Lox recombination method to produce non-functional FGF23. The nonfunctional FGF23 was confirmed by an intact FGF23 serum assay that showed undetectable serum FGF23 in these mice. FGF23-KO mice present with severe growth retardation, short life span, infertility and ectopic calcification [24] due to the fact that without FGF23, renal NPT2a cannot be down-regulated in response to increasing serum phosphate. Thus, these phenotypes are caused by highly elevated phosphate levels and subsequent biochemical dysregulation. FGF23 overexpressing mice manifest hypophosphatemia, osteomalacia and disturbed growth plate [14], mimicking ADHR and XLH patient phenotypes. This is consistent with the elevated FGF23 in this mouse model. α KL-KO mice share the same phenotypes with FGF23-KO mice [25] due to the fact that α KL deficiency leads to FGF23 signaling ablation, similar to a patient with α KL loss of function mutations.

Disorders involving phosphate metabolism

Phosphate is one of the most abundant elements in the human body. Maintaining proper concentrations is essential for normal bone mineralization and cellular biological functions, such as activity of kinases and the production of ATP and nucleic acids. Any alterations that happen during phosphate absorption, reabsorption or secretion may cause hypophosphatemia or hyperphosphatemia, and respective clinical features. While the mechanism of how phosphate is regulated has not been understood completely, recent studies of phosphate disorders have given us clues, especially the inherited disorders. Mendelian diseases are a good tool to gain insights into the genes which cause phosphate misregulation. The primary heritable phosphate disorders are listed in Table 1, and below is an introduction to these diseases.

Autosomal Dominant Hypophosphatemic Rickets (ADHR)

ADHR is a rare hereditary disease. The clinical presentations are low serum phosphate, up-regulated FGF23 levels and inappropriate low or normal circulating $1,25(\text{OH})_2\text{D}_3$. Presentation can be variable; with childhood onset, patients may present with severe clinical features, such as rickets and deformation of the lower extremities. Patients who present in adulthood may have bone pain and less severe fractures. In addition, ADHR can be incompletely penetrant, as unaffected carriers have been observed [26].

The FGF23 gene was first identified in ADHR as the causative gene (see FGF23 section). In ADHR, a subtilisin-like proprotein convertase (SPC) protease motif (R₁₇₆XXR₁₇₉) is mutated, which prevents the cleavage of FGF23 protein [10]. Normally, full length FGF23 can be cut into two fragments, a 20kD N-terminal portion and a 12kD C-terminal portion. In animal studies, these three different FGF23 forms were given to mice, and only the intact form caused phosphate reduction, indicating that full length FGF23 is the active form [11]. Also, in ADHR patients with severe features, the intact FGF23 levels are markedly elevated [27]. Thus this protease cleavage resistance leads to gain of function for the FGF23 protein.

The animal model for ADHR is a mouse model carrying the R176Q mutation in the FGF23 gene. To achieve classic ADHR clinical features, R176Q mice were put on an iron deficient diet which enhanced the FGF23 concentration changes. As iron depletion can cause increasing FGF23 expression in bone [28], R176Q mice on this special diet developed osteomalacia with hypophosphatemia and an elevated FGF23 level, due to this FGF23 cleavage resistance.

X-Linked Hypophosphatemic Rickets (XLH)

XLH is an X-linked dominant disorder, the most common inherited disease for osteomalacia, and has similar phenotypes to ADHR. Manifestations usually present during the first few years of life due to rapid growth: lower-extremity bowing, and clinical features of rickets and fracture. Lab findings include hypophosphatemia,

inappropriate normal $1,25(\text{OH})_2\text{D}_3$, with calcium and PTH often in the normal ranges [29]. Inactivating mutations in PHEX (Phosphate-regulating gene with homologies to endopeptidases on the X chromosome) are the cause of this disease. The PHEX protein product is a membrane bound metalloprotease, suggesting it functions to cut small peptides [30].

PHEX is primarily produced in bone cells, whereas its mutations cause phosphate wasting resulting from impaired reabsorption in the kidney. This suggests that PHEX interacts with hormonal factors outside of bone that act on kidney. In XLH patients, increased intact FGF23 has been observed [31]. In addition, the Hyp mice, a mouse model of XLH, were tested for its bone FGF23 mRNA expression and serum FGF23 concentration, which were also elevated [32], indicating that the PHEX mutation and FGF23 increases are related.

As mentioned above, the Hyp mouse model mimics the phenotypes of XLH with low serum phosphate, elevated FGF23, inappropriate $1,25(\text{OH})_2\text{D}_3$, and normal calcium. In Hyp mice part of the sequence on the 3' end of the PHEX gene has been deleted, so that no functioning PHEX can be produced in this mouse model [33].

Autosomal Recessive Hypophosphatemic Rickets (ARHR)

ARHR is characterized by phosphate wasting, increased FGF23, along with rickets and osteomalacia [3]. There are three types of ARHR. Type 1 is caused by an inactivation of

the gene Dentin Matrix Protein-1 (DMP1). Mutations lead to impaired osteocyte maturation resulting in FGF23 mRNA and protein level increases, which cause pathological changes of bone formation [34]. Ectonucleotide pyrophosphatase/phosphodiesterase-1 (ENPP1) recessive mutations are the cause for type 2 ARHR. Dysfunction of ENPP1 protein results in defective osteoblast differentiation and FGF23 expression elevations, leading to the ARHR phenotype [35] [36]. Type 3 ARHR is caused by Family with sequence similarity 20, member c (FAM20c) gene mutations. This mutation occurs in a kinase, and causes stabilization of FGF23 through reduced protease cleavage of the intact form.

Hyperphosphatemic Familial Tumoral Calcinosis (hFTC)

hFTC is an inherited autosomal recessive disease of over-phosphate reabsorption. It is characterized by ectopic calcium and phosphate deposition, which can be found in soft tissues and vessels. Biochemical findings include hyperphosphatemia due to increasing phosphate reabsorption, inappropriate normal $1,25(\text{OH})_2\text{D}_3$ with serum calcium and PTH in the normal ranges [37].

There are multiple mutations that cause hFTC. Polypeptide N-acetylgalactosaminyl transferase-3 is encoded by the GALNT3 gene and was the first identified hFTC mutation. This protein transfers a galactosamine to the hydroxyl group of a serine or threonine residue. In hFTC patients with GALNT3 mutations, elevated C-terminal FGF23 and reduced intact FGF23 have been observed [38]. This is due to diminished glycosylation

in the FGF23 R₁₇₆XXR₁₇₉ protease motif, which usually occurs at T₁₇₈, resulting in FGF23 instability and subsequent degradation [39]. *FGF23* destabilizing mutations or alpha-Klotho (α KL) loss of function mutations can also cause hFTC. The mutations in FGF23 lead to protein degradation, which is similar to the GALNT3 mutation effects on FGF23 protein. Since α KL is the co-receptor for FGF23 binding, α KL mutations can result in loss of FGF23 signaling, leading to severe hFTC phenotypes.

Chronic Kidney Disease (CKD)

CKD is a worldwide health problem due to its high prevalence, affecting 1 in 8 in America [40] with lethal complications. In CKD, kidney function loss caused by a wide range of renal injuries or genetic factors, including diabetes and high blood pressure. As the kidneys are the central organs for phosphate excretion, glomerular filtration rate (GFR) decreases paralleled with loss of nephrons results in phosphate retention and hyperphosphatemia. Loss of renal function also causes other biochemical abnormalities, like elevation of serum FGF23 and PTH, reduction of vitamin D metabolism, and decreasing calcium concentration. These pathological changes impact normal mineral metabolism, causing bone disease, ectopic calcification and cardiovascular diseases, which are lethal complications of CKD [41].

In CKD patients, nephron loss induces less active vitamin D production and less secretion, causing hypocalcemia and high serum phosphate. As a major mediator for PTH, low calcium level initiates secondary hyperparathyroidism. High PTH levels elevate

phosphate concentrations even further through bone turnover. With disease progression, FGF23 and PTH are elevated to act on remaining nephrons to compensate the biological function of the damaged kidney. In the advancing CKD stages, FGF23 concentrations are correlated with disease severity [42]. In addition, highly elevated serum FGF23 in CKD can be associated with cardiac alterations in patients undergoing hemodialysis [43].

In summary, phosphate balance is essential for normal development, cell function and skeletal homeostasis. Phosphate regulation is complex and regulated by various factors: chief among these is FGF23. In inherited diseases of phosphate metabolism, although these disorders have different causative genes, most of them involve FGF23 over-production or signaling impairment. Besides rare diseases, FGF23 also plays an important role in common diseases, like CKD. Thus it is important to study FGF23 and its signaling cascades towards developing new treatments.

Table 1 Primary inherited phosphate disorders involving FGF23

| Inherited Disease | Biochemical abnormalities | Causative Gene (Genes) | Type of mutation |
|---|----------------------------------|-------------------------------|-------------------------|
| Autosomal Dominant Hypophosphate Rickets (ADHR) | Hypophosphatemia | FGF23 | Gain of function |
| X-linked Hypophosphatemic Rickets (XLH) | Hypophosphatemia | PHEX | Loss of function |
| Autosomal Recessive Hypophosphatemic Rickets (ARHR) | Hypophosphatemia | DMP1 ENPP1 FAM20c | Loss of function |
| Familial Tumoral Calcinosis (FTC) | Hyperphosphatemia | GALNT3 FGF23 KL | Loss of function |

Hypothesized molecular pathway for FGF23 activity in kidney

Gene expression changes after FGF23 administration

As described above, the biological outcomes of FGF23 delivery occur in the kidney proximal tubules, decreasing phosphate absorption by mediating Npt2a internalization and reducing active vitamin D synthesis by down regulating the kidney $1\alpha(\text{OH})\text{ase}$ [5, 14]. The mechanisms of how the FGF23 signals communicate between the DCT and the proximal tubules (PT) is still not clear.

To study gene expression changes in the FGF23 signaling pathway, microarray chip technology was performed previously in the laboratory. Wild type (WT) mice were i.p. injected with either 10 μg recombinant FGF23 or vehicle (saline) and sacrificed after 1 hour. Kidneys were collected, kidney RNA was isolated and gene (mRNA) expression was tested by microarray. The expression of ninety-one genes was increased significantly ($p < 0.001$), and the most elevated nine genes are listed in Table 2.

Hypothesis for HBEGF participation in FGF23 signaling

It was previously demonstrated that FGF23 acts on the DCT to activate the MAPK pathway, which leads to increased Egr1 expression [44]. As expected, Egr1 gene expression showed approximately a 9-fold increase in the kidneys of FGF23 treated mice compared with the control groups. The genes highlighted in orange in Table 2 were

previously demonstrated being related to FGF23 signals [45] [46]. In the gene array, heparin-binding EGF-like growth factor (HBEGF) was the second-most up-regulated gene with a 3-fold increased expression, suggesting HBEGF might be a potential mediator conducting communication between the DCT and the PT.

In addition, HBEGF has been identified as a paracrine factor located in the kidney DCT [47]. Although HBEGF has not been previously associated with phosphate regulation, members of EGF family are found to participate in kidney electrolyte handling. In this regard, the fine excretion of magnesium takes place in the DCT due to autocrine effects of the factor epidermal growth factor (EGF). Pro-EGF protein becomes solubilized after proteolysis, which binds to the EGFR located on the same DCT cell, thus stimulating downstream signals to regulate magnesium channels. Loss of function mutations in EGF causes isolated recessive renal hypomagnesemia (IRH), a disease of magnesium wasting [48]. Thus, as a member of EGF family, HBEGF may also play a role in phosphate regulation as a paracrine factor to communicate the signals between the DCT and PT.

| Gene Name | Symbol | NCBI No. | Fold Change | P-value |
|---|---------------|-----------|-------------|----------|
| Early growth response 1 | <i>Egr1</i> | NM_007913 | 9.067 | 2.45E-08 |
| Heparin-binding EGF-like growth factor | <i>Hbegf</i> | NM_010415 | 3.097 | 3.98E-05 |
| Dual specificity phosphatase 6 | <i>Dusp6</i> | NM_026268 | 2.417 | 1.49E-09 |
| Zinc finger protein 36 | <i>Zfp36</i> | NM_011756 | 2.224 | 0.000470 |
| Immediate early response 2 | <i>IER2</i> | NM_010499 | 1.967 | 1.26E-05 |
| Dual specificity phosphatase 4 | <i>Dusp4</i> | NM_176933 | 1.878 | 0.001636 |
| Basic helix-loop-helix domain, class B2 | <i>Bhlhb2</i> | NM_011498 | 1.797 | 0.000296 |
| Nab2 // Ngfi-A binding protein | <i>Nab2</i> | NM_008668 | 1.699 | 0.000446 |
| Junb // Jun-B oncogene | <i>c-Jun</i> | NM_008416 | 1.655 | 0.000557 |

Table 2 Kidney microarray data after acute FGF23 administration

An hour post injection of FGF23 in mice showed a significant change in kidney mRNA expression compared to control injected mice by microarray. The top nine genes are listed in the table with *Egr1* serving as the positive control for the FGF23 signaling event. HBEGF was the second-most highly elevated gene, which might suggest its significance in the FGF23 signaling pathway.

[Figure courtesy: Dr. Kenneth White]

General properties of HBEGF

Heparin-binding EGF-like growth factor (HBEGF) is a member of the EGF family. First identified from human macrophages, it is capable of stimulating differentiation of smooth muscle cells and fibroblasts and has heparin affinity [49]. The human HBEGF gene is located on chromosome 5 and contains 6 exons, encoding HBEGF protein composed of 208 amino acids in its full-length form (pre-proHBEGF) [50]. Pre-pro-HBEGF is a single transmembrane protein, whose maturation undergoes several proteolytic steps. It is firstly cleaved by a furin-like enzyme between amino acids 62 to 63 to produce a pro-HBEGF. Then pro-HBEGF is most likely cut by a disintegrin and metalloproteinase (ADAM), resulting in a mature soluble HBEGF (sHB) (see Figure 4) [51]. In pro-HBEGF and sHB, the EGF-like domain is most likely the key motif for EGFR recognition [52]. The cytoplasmic fragment also has a biological function in cellular proliferation in an EGFR-independent manner [53].

HBEGF processing and signaling

The ADAMs proteases are induced through G-protein coupled receptor activation, and these proteolytic enzymes cut pro-HBEGF close to the cell surface, causing ectocellular shedding. Then sHB acts as autocrine, paracrine or juxtacrine factor to bind ErbB1/HER1 and ErbB4/HER4, two members of the EGF receptor family, to activate the receptors' intracellular tyrosine kinase domains, and elicit signal cascades, such as MAPK and NF- κ B [54] [55].

Within the ADAM family, ADAMs 10 and 17 are thought to be the main enzymes for HBEGF shedding. In addition, cells with deficient ADAM17 can be rescued by adding ADAM10, while ADAM10 only functions when ADAM17 is absent [56]. In animal studies, mice lacking ADAM17 mimic the phenotype of growth factor knockout mice, which are lethal before birth [57].

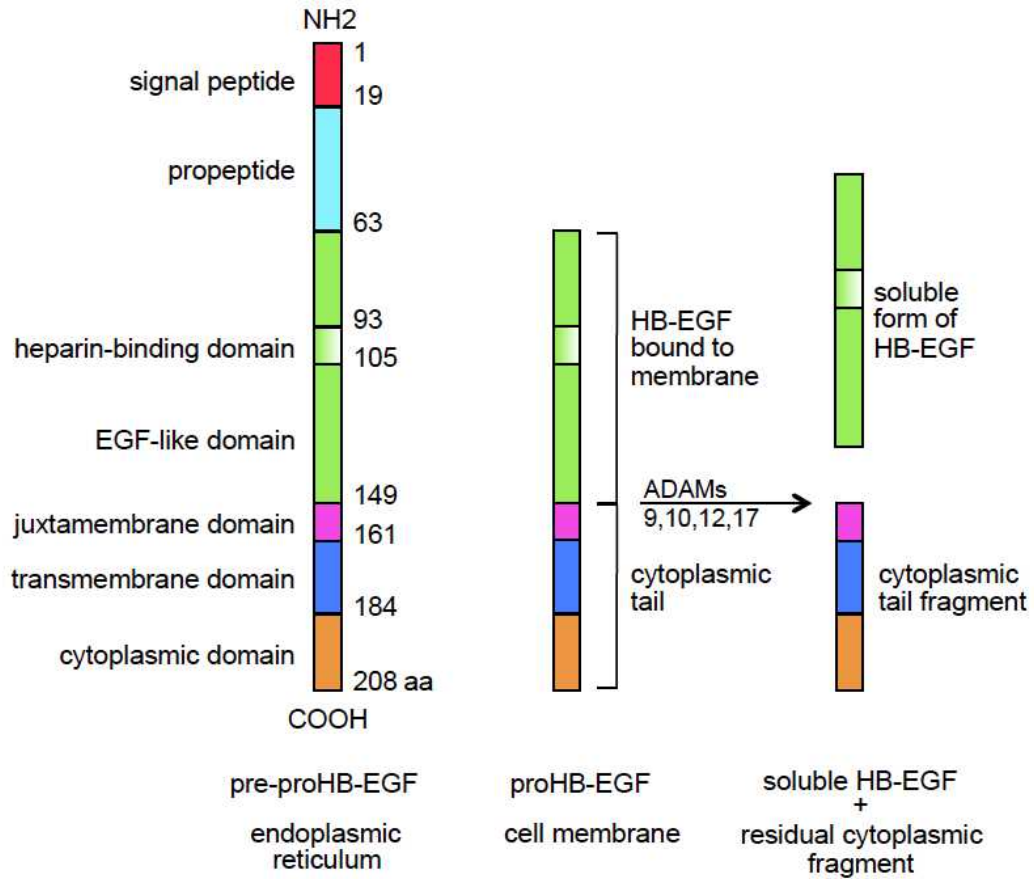


Figure 4 Structure and processing of HBEGF

The pre-pro-HBEGF is the full length HBEGF. After being cut by a furin-like protease, it becomes pro-HBEGF. Then ADAMs cleave the pro-HBEGF form into sHB and the cytoplasmic form of HBEGF.

[Figure adapted from [51]]

Global Hypothesis

In the present studies, I tested whether HBEGF is involved in electrolyte regulation, similar to EGF's function. Because HBEGF is up regulated following FGF23 delivery, I hypothesized that this factor stimulates the renal PT to mediate FGF23-dependent phosphate homeostasis (see Figure 5). In this regard, I performed *in vivo* experiments testing HBEGF activity in mice devoid of FGF23 or its signaling components (Klotho), developed and characterized an anti-HBEGF antibody, tested an *in vitro* assay, and examined the localization of FGF23 and HBEGF signaling *in vivo*.

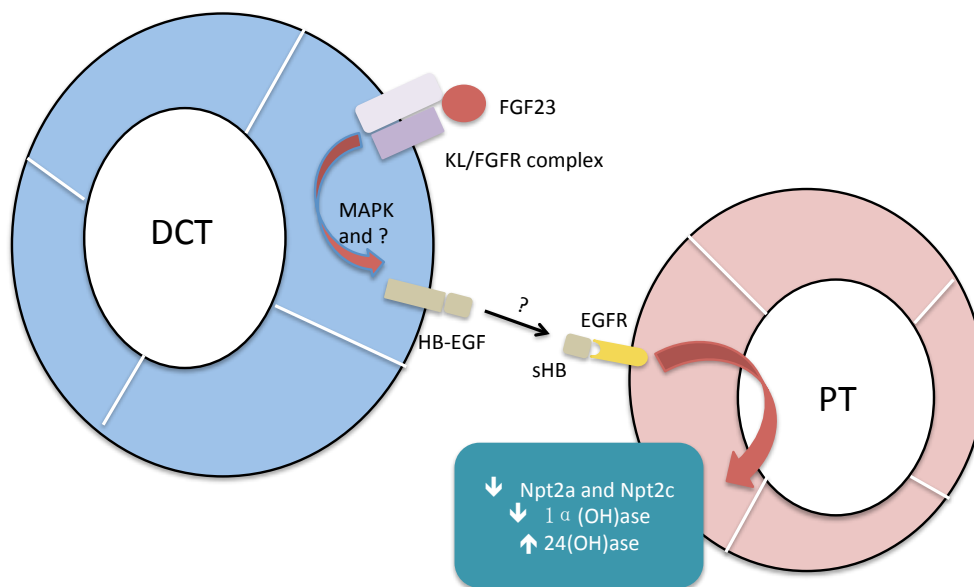


Figure 5 FGF23 hypothesized downstream signaling

This is a diagram for FGF23 signaling and a hypothesized pathway of how FGF23 passes its signals from DCT to PT. In this regard, it is hypothesized that FGF23 signals in the renal DCT and some unknown downstream signaling (the question mark in the DCT) leads to the cleavage of HBEGF. sHB may travel to the PT (the question mark between two tubules) and affect the activities in the renal PT on NPT2a and 1,25D synthesis.

Materials and Methods

Animal Studies

Animal studies were performed according to the Institutional Animal Care and Use Committee for Indiana University, and comply with the NIH guidelines.

For immunofluorescence studies, recombinant HBEGF (10 μ g), recombinant FGF23 (10 μ g) and vehicle (100 μ l saline) were delivered to 12-week old WT mice through tail-vein injections. Mice were euthanized after ten minutes. Kidneys were perfused by saline and then fixed by 4% paraformaldehyde (PFA), and then submerged in 4% PFA in microcentrifuge tubes (Midwest Scientific, MIDSCI) overnight.

For gene expression studies, 6-8 week old mice (FGF23-KO mice, α KL-KO mice [25] and WT mice) were i.p. injected with 10 μ g HBEGF, 10 μ g FGF23, 100 μ l vehicle (saline), then sacrificed after one hour. Serum was collected first, and then followed by saline perfusion, PFA fixation and tissue harvesting: one kidney for immunofluorescence staining, half kidney for RNA extraction, half kidney for protein collection and serum.

The FGF23 KO mouse is a conditional knockout mouse model generated by our laboratory. In this model, FGF23 exon 2 was deleted using a ubiquitous EIIa - Cre Lox recombination system [24].

Cell Culture

An mKL cell line [23], HEK293 cells stably transfected with mKL, were cultured in DMEM/F-12 (Hyclone) supplemented with 10% fetal bovine serum, 1% sodium pyruvate (ThermoFisher Scientific), 1% L-Glutamine 100X Solution (Hyclone), 50,000U Penicillin-Streptomycin Solution (Hyclone), 450ug/ml Geneticin (G-418, ThermoFisher Scientific); cells were incubated at 37°C and 5% CO₂. Medium was changed every 2 to 3 days.

Transient transfection for immunoblotting and qPCR

5 x 10⁵ mKL cells were seeded on a collagen I coated 6-well plate (Thermo Scientific Nunc) for each well. After 20 hours incubation, cells were transfected with 3.3 µg of plasmid DNA in 153ul DMEM/F-12 with 12ul of FuGENE HD reagent (Promega) per well.

Transient transfection for immunofluorescence

1 x 10⁵ mKL cells were seeded on 4-well CultureSlides with a uniform application of rat tail collagen type I (Corning BioCoat) and incubated for 20 hours. Then cells were transfected with 0.55ug of plasmid DNA in 26ul DMEM/F-12 with 1.7ul FuGENE HD reagent following the protocol.

Cell treatments

24 hour post-transfection, cells were changed to serum free media, and treated with vehicle (saline), 500ng/ml recombinant FGF23 or 2nM TPA for different time points: 1h, 6h, 24h.

Immunoblotting

Cell lysate preparation

mKL cells were washed twice with PBS, lysed with 200ul 1X cell lysis buffer (Cell Signalling) with 0.1% 4-(2-Aminoethyl) benzenesulfonyl fluoride hydrochloride (AEBSF, Santa Cruz), collected in 1.7ml microcentrifuge tubes (MIDSCI). Samples were kept at -20°C for later use.

Gel electrophoresis and transfer

Samples were thawed on ice and centrifuged one minute at maximum speed. Then the protein concentration was measured by the Coomassie Plus (Bradford) Assay kit (Thermo Scientific). Sample loading volumes were calculated to ensure equal protein amounts. An equal volume of freshly made Laemmli Sample Buffer (Bio-Rad) with 5% β -mercaptoethanol/2-Mercaptoethanol (β -ME, Fisher-Scientific) was added to the cell lysate samples and boiled for five minutes. After cooling down to room temperature,

samples were electrophoresed on AnyKD Mini-Protean TGX Gels (Bio-Rad) and transferred to a PVDF membrane (Bio-Rad) for 3 minutes using a Trans-Blot Turbo transfer system (Bio-Rad).

Western Blotting

Membranes were blocked in 5% dry milk powder (Scientific Inc) in 1XTBS (Tris-buffered saline, Bio-Rad) for one hour at room temperature, followed by primary antibody incubating at 4°C overnight (see Table 3 for concentrations). Membranes were rinsed three times, ten minutes each, in 1XTBS with 0.05% Tween 20 (USB Corporation). Then the membranes were incubated in secondary goat anti-rabbit IgG-HRP conjugate (Bio-Rad) antibody at 1:5000 to 1:10000 dilution for one hour (see Table 4 for concentrations). Enhanced chemiluminescent (ECL, GE Healthcare) was used to detect horseradish peroxidase (HRP) activity and membranes were exposed to X-ray films.

Table 3 Primary antibodies for WB

| Primary Antibody for Western Blotting | Vendor | Dilution |
|--|----------------|-----------------|
| EGF Receptor (D38B1) | Cell Signaling | 1:1000 |
| Phospho-EGF Receptor (Try1068) | Cell Signaling | 1:800 |
| ERK1/2 | Promega | 1:5000 |
| Phospho-p44/42 MAPK (Erk1/2) | Cell Signaling | 1:1000 |

Table 4 Secondary antibodies for WB

| Secondary Antibody for Western Blot | Vendor | Dilution |
|--|---------------|-----------------|
| Goat Anti-Rabbit IgG-HRP Conjugate | Bio-Rad | 1:5000-1:10000 |
| Donkey Anti-Goat IgG-HRP | Santa Cruz | 1:3000 |

Immunofluorescence

Cell staining

After transfection as described above, cells were treated with recombinant human FGF23 500 ng/ml or saline as control for 1, 6 or 24 hours. Cells were washed two times with PBS (Hyclone), and fixed in 4% paraformaldehyde (PFA) for 15 minutes. Cells were then blocked with 10% goat serum with 0.2% Triton X-100 (Sigma) in PBS (blocking buffer) for 1 hour at 37°C in a humidity chamber. All the following incubation steps were performed in a humidity chamber. Primary antibody (see Table 5 for dilution) was diluted in blocking buffer and added to slides for incubation at 4°C overnight. Then slides were rinsed three times in PBS with 0.2% Triton X-100. After rinsing, secondary antibody (see Table 6 for dilution) was added at 1:250 dilution in blocking buffer to the slides, and incubated in the dark at room temperature for 1 hour followed by rinsing three times. Slides were mounted with media containing DAPI (Vector Laboratories) to stain nuclei, and observed with a Leica DM5000B fluorescent microscope.

Table 5 Primary antibodies for IF

| Primary Antibody for Immunofluorescence | Vendor | Dilution |
|--|----------------|-----------------|
| Klotho KO603 | TransGenic Inc | 1:20 |
| Phospho-p44/42 MAPK (Erk1/2) | Cell Signaling | 1:50 |

Table 6 Secondary antibodies for IF

| Secondary Antibody for Immunofluorescence | Vendor | Dilution |
|--|---------------|-----------------|
| Alexa Fluor 488 Goat anti-Rabbit | Thermo Fisher | 1:200 |
| Alexa Fluor 594 Goat anti-Rabbit | Thermo Fisher | 1:200 |
| Goat anti-Rat IgG Alexa Fluor 488 Conjugate | Thermo Fisher | 1:200 |
| Goat anti-Rat IgG Alexa Fluor 594 Conjugate | Thermo Fisher | 1:200 |

Tissue staining

At necropsy, mice were perfused with saline and then 4% PFA through the systemic circulation before removal. Kidneys remained in 4% PFA at 4°C for 24 hours, washed in PBS and then incubated in 30% sucrose for 48-72 hours at 4°C. Kidneys were embedded in O.C.T. (Sakura Finetek) and frozen at -80°C. Tissues were sectioned at 8 µm using Leica cryostat at -20°C and placed on slides. Samples were kept at -80°C for long-term storage.

Staining protocol

Slides were kept at room temperature for 20 minutes to let the O.C.T. dry. Sections were circled using a hydrophobic barrier pen (Fisher Scientific), then antigen retrieval was performed using pepsin (Carezyme II: Pepsin, Biocare Medical) for 5 minutes at 37°C. Slides were rinsed three times, five minutes each in PBS. Image-iT FX Signal enhancer (Thermo Fisher) was added to slides for 30 minutes at room temperature for blocking background signals, followed by three rinses in PBS. 1 hour additional blocking was performed using 10% goat serum in 0.2% Triton X-100 in PBS (blocking buffer) at 37°C. After blocking, primary antibody (see Table 4) was added on slides diluted in blocking buffer for incubation at 4°C overnight. Slides were rinsed three times thoroughly in 0.2% Triton X-100 in PBS (washing buffer) for ten minutes. After rinsing, appropriate fluorescent secondary antibody was added, diluted in blocking buffer, and slides were incubated for one hour in the dark at room temperature. Slides were rinsed three times ten minutes each, and mounted with DAPI mounting media (Vector Laboratories) or Prolong Gold Antifade Mountant (ThermoFisher Scientific). Images were taken with a DM5000B fluorescent microscope (Leica Microsystems). All incubations were performed in a humid chamber.

Quantitative PCR

Tissue RNA Preparation

Kidney samples were collected in TRIZOL (Invitrogen) and homogenized using Navy Rino Bullet Blender tubes (MIDSCI) in a Bullet Blender (Next Advance). RNA was extracted following the TRIZOL Reagent protocol.

Cell RNA Preparation

Cell RNA extraction was performed using the RNeasy Mini kit (Qiagen, Inc.). Cells were washed three times with PBS, then 350 μ l buffer RLT (lysis buffer) with 3.5 μ l β -ME was added to each well. After cells were collected and mixed well in RLT buffer, they were transferred to microcentrifuge tubes. RNA was extracted following the RNeasy Mini protocol for purification of total RNA from animal cells using microcentrifuge columns according to standard Qiagen, Inc. protocols.

Real Time PCR (q-PCR)

Samples were tested using mouse or human primers for 1- α OHase, 24-OHase, Egr1 and the control β -actin (see Table 6). After RNA extraction, 10 ng/ μ l RNA dilution was made in RNase free water. For each well, 12.5 μ l TaqMan RT-PCR Mix (2X), 0.625 μ l TaqMan RT Enzyme Mix (40X), 0.375 μ l RNase free water, 0.5 μ l 10 μ M forward primer, 0.5 μ l

10 μ M reverse primer and 0.5 μ l 5 μ M probe were added in a MicroAmp Optical 96-well reaction plate (Applied Biosystems). The quantitative PCR conditions were: 30 min 48°C, 10 min 95°C, followed by 40 cycles of 15 sec 95°C and 1 min 60°C. Then data was collected using the comparative C_T ($\Delta \Delta C_T$) experiment workflow according to the StepOnePlus Real-Time PCR System (Thermo Fisher). Each sample was analyzed in duplicate, and the fold change of each gene expression was tested by the 2^{- $\Delta\Delta C_T$} method.

Table 7 Real-time PCR Primers

| Gene | Forward Primer | Reverse Primer | Probe | Vendor |
|------------------|------------------------------------|--------------------------------------|--|---------------|
| Mouse Actin | 5'-GGCTCCTAG CACCATGAAG- 3' | 5'-ACCGATCCA CACAGAGATCT -3' | 5'-FAM- TCAAGATCA TTGCTCCTCCT GAGCGC- TAMRA-3' | IDT |
| Mouse EGR1 | 5'-AGCCGAGCG AACAACCCTAT -3' | 5'-CGCCTTCTC ATTATTCAGAG CG-3' | 5'-FAM- AGCACCTGA CCACAGAGTC CTTTTCTGACA -TAMRA-3' | IDT |
| Mouse 24OHase | 5'-GGCCTGGGA CACCATTTTC-3' | 5'-GCTGGGAAT ATCTCTCTAGG CG-3' | 5'-FAM- AATCAGTCA AGCCCTGCAT CGACCA- | IDT |

| | | | | |
|------------------|-----------------------------------|--|--|-----|
| | | | TAMRA-3' | |
| Mouse 1aOHase | 5'-AGGCTGCAT GAACTGCAGG- 3' | 5'-TCCCAAAGC TGCCAGACC-3' | 5'-FAM- CATGGCGCT- ZEN- GCGCGGTACG- IBFQ-3' | IDT |
| Human Actin | 5'-GGCACCCAG CACAATGAAG- 3' | 5'-GCCGATCCA CACGGAGTACT -3' | 5'-FAM- TCAAGATCA TTGCTCCTCCT GAGCGC- TAMRA-3' | IDT |
| Human EGR1 | 5'-GGACACGGG CGAGCAG-3' | 5'- CGTTG TTCAGA G AGATGTCAGGA -3' | 5'-FAM- CCTACGAGC ACCTGACCGC AGAGTCT- TAMRA-3' | IDT |

HBEGF antibody

A rabbit anti-mouse HBEGF antibody was made by GenScrip, USA, Inc. A 26 amino acid sequence, CLNLFKVAFSSKPQGLATPSKERNGK, of mouse HBEGF was chosen as the peptide for antibody generation in rabbits (see Results).

Other materials

Table 8 Recombinant Protein

| Protein Name | Vendor |
|---------------------|---------------|
| Human HBEGF | R&D Systems |
| Human FGF-23 | R&D Systems |
| Mouse HBEGF | Sigma |

Table 9 Other Chemicals

| Names | Vendor |
|---|-------------------|
| Fluorescein labeled Lotus Tetragonolobus Lectin (LTL) | Vectashield |
| Phorbol 12-myristate 13-acetate (TPA) | TOCRIS Bioscience |
| Heparin-agarose | Sigma Aldrich |
| β -mercaptoethanol | Fisher Scientific |

Statistical Analysis

Gene expression changes were analyzed by student t-test using raw data collected from StepOnePlus Real-Time PCR System. The change was considered significant when $p < 0.05$.

Results

Initial study of HBEGF activity *in vivo*

To investigate whether HBEGF plays a role downstream of the FGF23 signaling pathway in the kidney, *in vivo* studies were performed. As described above, FGF23 binds FGFR1 and co-receptor α KL on the DCT and activates the MAPK pathway. This signaling then initiates a reaction in the PT causing decreasing $1\alpha(\text{OH})\text{ase}$ expression and degradation of NPT2a [23]. Due to the gene array analysis and properties of corresponding proteins, we hypothesized that HBEGF was a potent paracrine factor required for FGF23 bioactivity. We used two mouse models that contained impaired FGF23 signaling to test if HBEGF supplementation could rescue the defects in phosphate homeostasis.

In α KL-KO mice, which lack Klotho gene expression, the FGF23 signaling pathway is impaired due to the lack of the obligate FGF23 co-receptor. When FGF23 is unable to activate its downstream reactions, $1\alpha(\text{OH})\text{ase}$ expression is aberrantly increased, thus $1\alpha(\text{OH})\text{ase}$ mRNA levels were used as a marker of FGF23 signaling activity. To identify if HBEGF could rescue FGF23 signaling in α KL-KO mice, 10 μ g recombinant HBEGF or vehicle was injected intraperitoneally in α KL-KO mice (eight mice for each group), and vehicle was injected in four WT mice (Figure 6). Mice were sacrificed 1 hour later, and kidneys were collected for q-PCR analysis of mouse $1\alpha(\text{OH})\text{ase}$ and mouse actin gene expressions.

Due to the α KL co-receptor deletion, vehicle injected α KL-KO mice showed 18-fold higher $1\alpha(\text{OH})\text{ase}$ mRNA levels compared to WT controls; p-value was 0.0039. Whereas in HBEGF treated mice, the injection led to a 10-fold reduction of $1\alpha(\text{OH})\text{ase}$ mRNA compared with vehicle treated α KL-KO mice with a 0.0273 p-value, even though $1\alpha(\text{OH})\text{ase}$ expression was still significantly elevated more than in WT controls. This significant reduction demonstrated that recombinant HBEGF rescued the FGF23 defective signaling activity.

In parallel experiments, FGF23-KO mice were used. As exon 2 of FGF23 was deleted in these FGF23-KO mice, there was no FGF23 produced, resulting in hyperphosphatemia. To determine if HBEGF could rescue this loss of FGF23, FGF23-KO mice were injected with vehicle (saline or 'sal'), 10 μ g recombinant HBEGF or 10 μ g recombinant FGF23 (Figure 7). There were three mice in the KO-sal group (FGF23-KO mice injected with vehicle), three mice in KO-FGF23 group (FGF23-KO mice injected with FGF23), six mice in KO-HB group (FGF23-KO mice injected with HBEGF) and six mice in WT-sal group (wild type mice injected with vehicle). Mice were euthanized one hour post-injection and kidneys were collected for q-PCR analysis for $1\alpha(\text{OH})\text{ase}$ gene changes.

Compared with WT control, $1\alpha(\text{OH})\text{ase}$ expression in the three FGF23-KO groups were significantly elevated due to non-functional FGF23 and the p-values for each comparison were 0.0432 (KO-sal v.s. WT-sal), 0.0299 (KO-FGF23 v.s. WT-sal) and 0.0051(KO-HB v.s. WT-sal). Within FGF23-KO groups, recombinant FGF23 suppressed $1\alpha(\text{OH})\text{ase}$ to

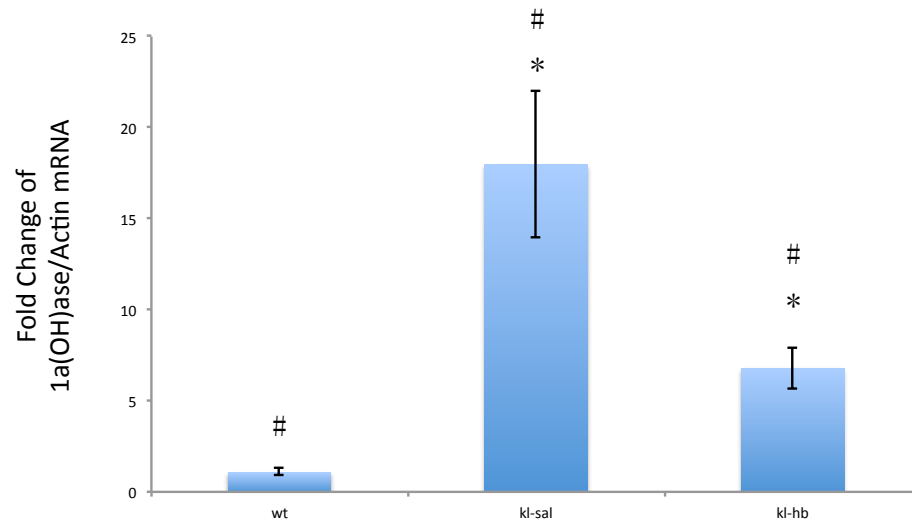


Figure 6 q-PCR analysis of HBEGF administration in α KL-KO mice

Wild type mice, injected with saline, as well as α KL-KO mice were injected with saline or 10 μ g recombinant HBEGF, then euthanized 1 hour later. Renal 1 α (OH)ase gene expressions were evaluated by real-time PCR. The reduction in KL-HB group was significant compared with KL-sal group, $p < 0.05$ (*). Both KL-HB and KL-sal groups had significant elevated 1 α (OH)ase gene expressions versus WT group, $p < 0.05$ (#). (n =4-8)

40-fold less versus vehicle injected mice (p-value was 0.0921). In addition, the KO-HB group showed robust decreased $1\alpha(\text{OH})\text{ase}$ expression with a 0.0767 p-value versus KO-sal, suggesting canonical FGF23 signaling cascade was partially regained due to sHB administration. Even though there was a decreasing trend compared to FGF23-KO saline treated mice, the reduction of $1\alpha(\text{OH})\text{ase}$ in FGF23 and HB injected FGF23-KO mice was not statistically significant; however, the trends mimicked the results in $\alpha\text{KL-KO}$ mice.

Therefore, the above *in vivo* studies strongly suggested that sHB regulated genes were associated with phosphate metabolism. HB mimicked FGF23 actions and rescued its biological activity in models where the FGF23 signaling pathway was impaired.

Therefore, these results are in agreement with the hypothesis that HB functions as a downstream mediator of the FGF23 pathway in the kidney. Like EGF, HBEGF could be potentially cleaved into a soluble form in this pathway and travel from the DCT to the PT mediating FGF23 activity.

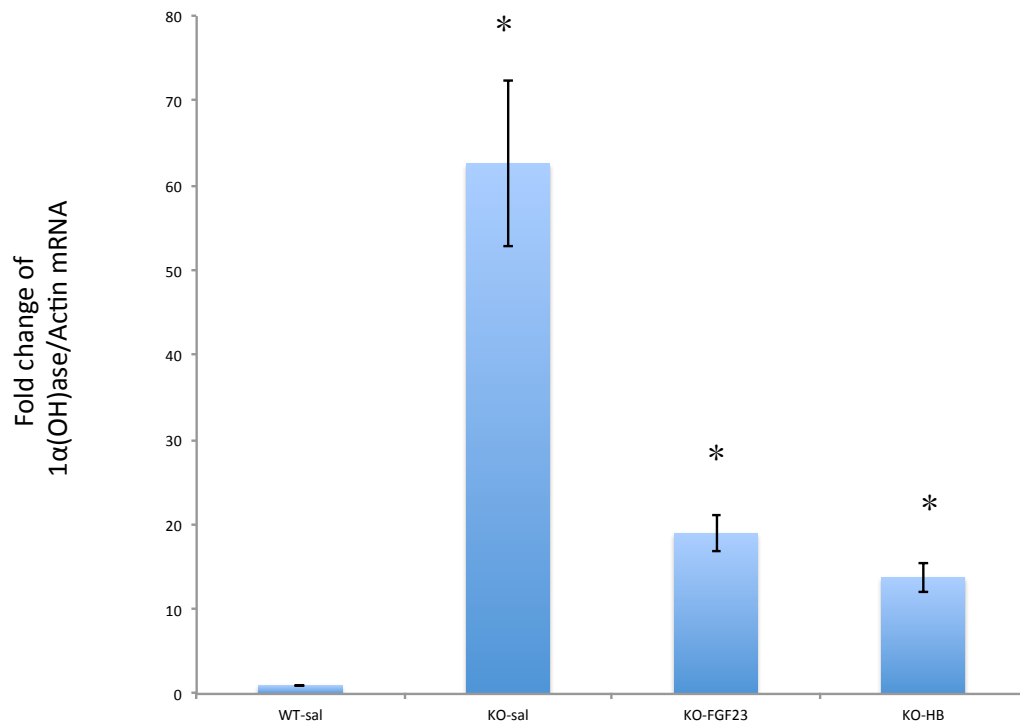


Figure 7 q-PCR analysis of HBEGF administration to FGF23-KO mice

FGF23-KO mice were injected with saline, 10 μg FGF23 or HBEGF. Wild type mice were injected with saline. Mice were euthanized 60 minutes later. Mouse 1α(OH)ase and mouse actin gene expression were evaluated by real-time PCR. Expression changes between FGF23-KO groups and WT control group were significant, $p < 0.05$ (*). 1α(OH)ase levels decreased between KO-FGF23 versus KO-sal and KO-HB versus KO-sal (were 0.092 and 0.077, respectively).

Preparation of an HBEGF antibody

To better understand how HBEGF functions in the kidney, it is important to obtain a high-quality mouse HBEGF antibody, which can be used for Western blots and immunofluorescence. Therefore polyclonal rabbit anti-mouse HBEGF antibodies were produced. Two New England rabbits (number 16435 and 16436 from GenScrip USA Inc) were immunized three times with recombinant HBEGF peptides (CLNLFKVAFSSKPQGLATPSKERNGK), a sequence from mouse HBEGF protein (Figure 8). The rabbits' sera were collected and probed against mouse recombinant HBEGF protein (Sigma) by Western blots (Figure 9a) to test if the immune injections were successful. The mouse recombinant HBEGF protein was a polypeptide chosen from the soluble HB (sHB) amino acid sequence. For conciseness, numbers "1" and "2" were used to replace the rabbits' company-provided numbers.

To test the antibody, immunoblots were first performed. The molecular mass of sHB is about 15 kD, whereas the membrane bound form is 22 kD. In Figure 9a, there was no band for sHB in pre-immune probing as expected. In immune serum probed membranes, sHB bands were clear in the 25 ng loading lane for both rabbits' sera, and some non-specific bands in number 2 rabbit's serum were apparent. After proving the antibodies' existence, serum was collected and purified. Purified antibodies were then tested on recombinant mouse sHB at different concentrations (Figure 9b), 0.5 $\mu\text{g/ml}$ and 1 $\mu\text{g/ml}$. Both conditions presented clear bands at 15 kD, the common mass for sHB. These results showed that the HBEGF antibody recognized HBEGF protein.

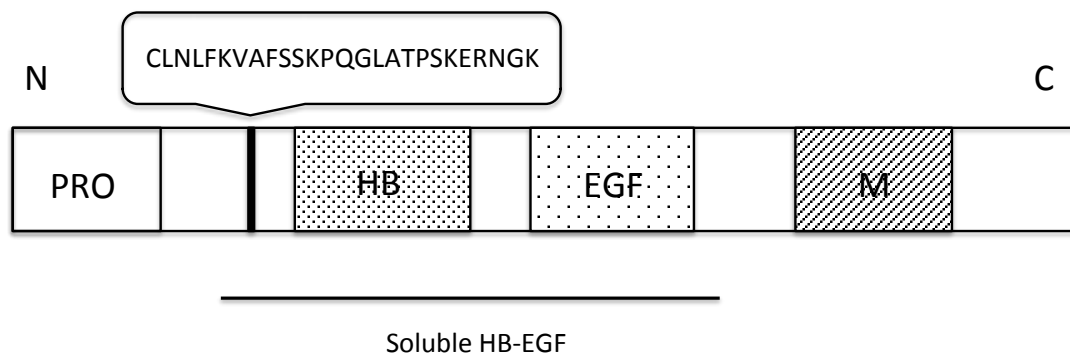


Figure 8 HBEGF structure and immune polypeptide

“M” refers to trans-membrane domain, “EGF” refers to EGF like fragment, “HB” refers to heparin binding fragment. The peptide chosen for immune is in the soluble HBEGF portion, but also contained in the membrane form.

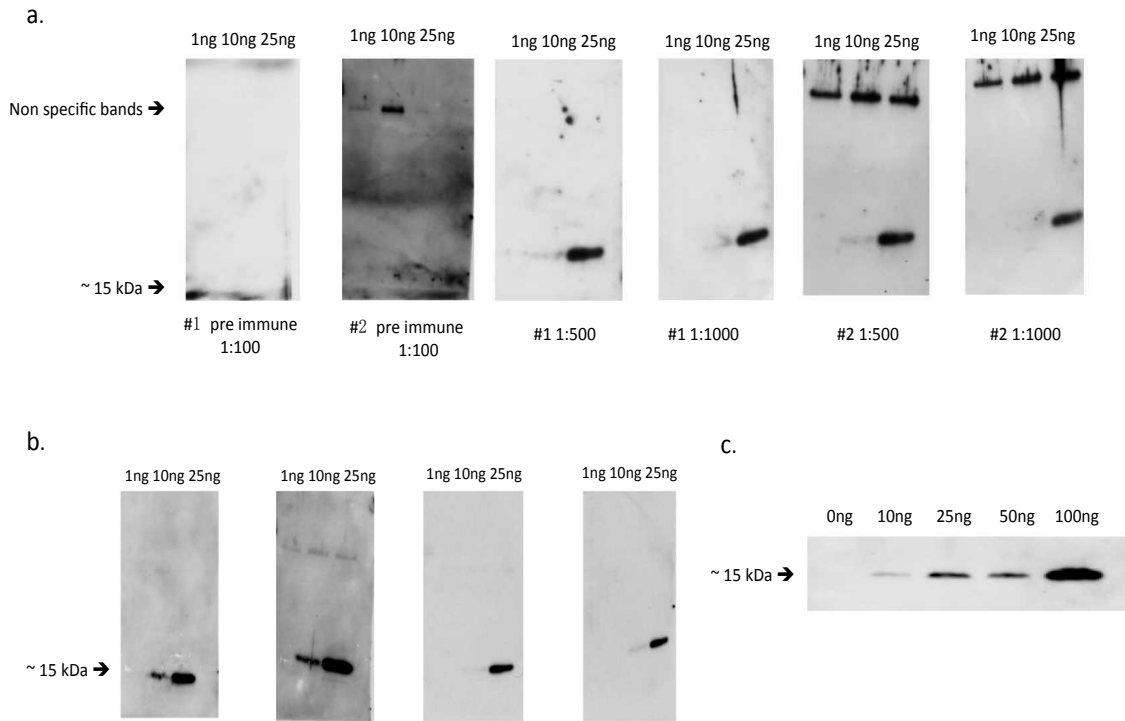


Figure 9 HBEGF antibody characterization

(a) Unpurified antibody tests: 1ng, 10ng and 25ng recombinant mouse HBEGF protein were added to each lane, and membranes were probed with two different pre-immune rabbit sera and unpurified immune sera. (b) Purified antibody tests: 1ng, 10ng and 25ng recombinant mouse HBEGF protein were added to each lane, and membranes were probed with two purified antibodies with different concentrations. (c) Anti-HBEGF antibody recognized recombinant HBEGF after purification with heparin-agarose.

Heparin-agarose purification of sHB was planned to be used as a future *in vivo* tissue collecting step. Thus, it would be important to assure the HBEGF antibody could recognize post-purification HBEGF protein. Recombinant mouse HBEGF protein was incubated with heparin-agarose overnight at 4°C. The protein was collected, then underwent immunoblot and was transferred to a membrane to be probed with the HBEGF antibody to ensure heparin-agarose purification would not disturb antigen-antibody binding. As shown in Figure 9c, the anti-HBEGF antibody recognized the heparin-purified recombinant HBEGF protein.

The next step was to use a cell model for testing the HBEGF antibody. The human embryonic kidney 293 (HEK293) cell line was used. These cells are relatively easy to grow and transfect with plasmids. HBEGF (HB DNA) and empty (pcDNA) plasmids were prepared previously in the laboratory (vehicle plasmid at 1499.3ng/μl, HB plasmid at 952.3ng/μl). Cells were seeded on plates or slides for 20 hours, then plasmids were transfected into the cells with FuGENE HD reagent. For Western blots, cell lysates and cell media were collected. To condense the media, heparin-agarose purification was used before immunoblots. As shown in Figure 10a, only the HB-transfected lysate lane had reacting bands, recognized by both HBEGF antibodies, within 15kD to 37kD range as this was likely the membrane bound form. sHB levels in the cell media were undetectable. The first lane was loaded with recombinant mouse sHB as a positive control. In Figure 10b, transfected cells were stained with the HB antibody to test the antibody's usefulness for immunofluorescence. Staining was observed in HBEGF transfected cells (green), but not in empty-plasmid transfected cells.

After these analyses, it was demonstrated that the HBEGF antibody recognized different forms of HB protein, both the soluble form on immunoblot and the membrane-bound form on cells. Thus this tool could be applied as a useful reagent to study HBEGF expression and bioactivity.

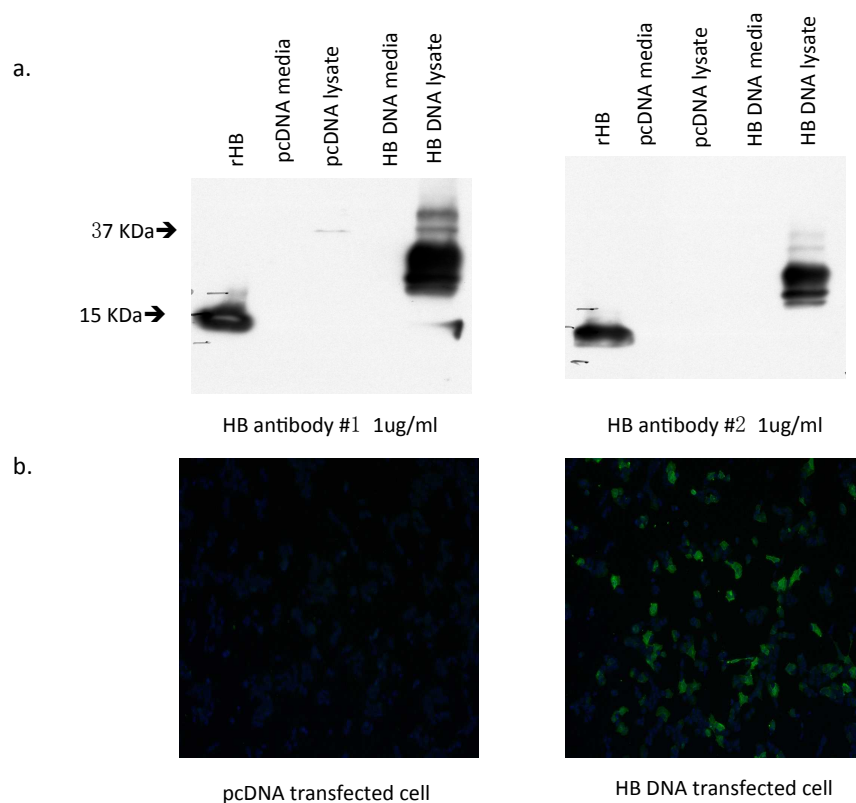


Figure 10 *In vitro* HBEGF antibody testing

(a) Western blots testing two HBEGF antibodies, the concentration was $1\mu\text{g/ml}$ for both. The first lane was loaded with mouse recombinant HBEGF protein and reacted at approximately 15 kD. The second and third lanes were empty plasmid (pcDNA) transfected cell media and cell lysates, and the fourth and fifth lanes were HBEGF transfected cell media and cell lysates. (b) Immunofluorescence for empty plasmid (pcDNA) transfected and HB transfected HEK293 cells, showing positive HB staining (green) as well as blue for nuclei.

***In vitro* model for HBEGF characterization**

In order to understand the mechanisms of how HBEGF works in FGF23 signaling pathways, an *in vitro* model was tested. The HEK293 cell line was chosen due to its high transfection rate. As this cell line did not express α KL or HBEGF, which were essential for FGF23 signaling, cells were transfected with mKL and/or HBEGF plasmids. Co-transfection of mKL and HBEGF was tested first, but due to its low transfection efficiency rate (figure not shown), we switched to an mKL cell line, which were HEK293 cells stably expressing mKL. This cell line was developed previously in the laboratory [23]. mKL cells were transfected with the HBEGF plasmid, and after 24 hours transfection cells were transferred to serum free media and adapted for 6 hours to ensure no interference by serum, then treatments were performed.

Figure 11 was the hypothesized signaling process for this cell model. After FGF23 administration, it would bind the receptor complex and activate downstream signals which including the MAPK pathway. An unknown mechanism might trigger HBEGF shedding through ADAM protease, allowing sHB to act like an autocrine or paracrine factor to bind its receptor, EGFR or ErbB4, and cause signaling actions. Potentially, MAPK pathways could also be activated downstream of HBEGF signals, as this factor is known to signal through the MAPK pathway.

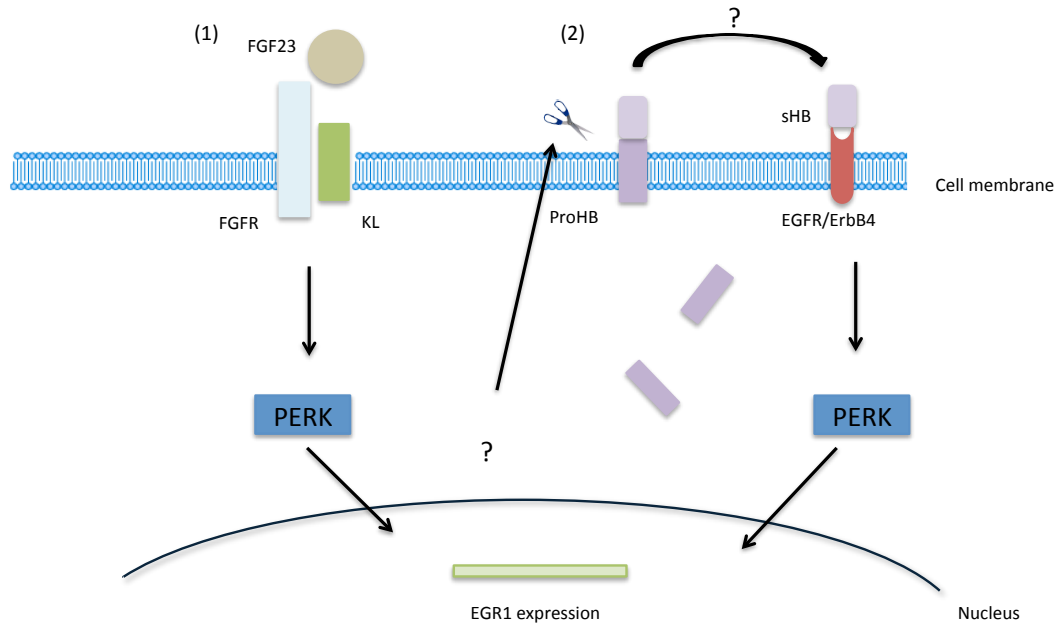


Figure 11 Hypothesized HBEGF signaling *in vitro*

In the mKL cell model, FGF23 activated its receptor and led to gene changes, including increased EGR1. It was hypothesized HBEGF could be proteolyzed after FGF23 signaled in the DCT cells through Klotho and FGFR1. (1) FGF23 binds its receptor complex (FGFR and α KL) and stimulates the MAPK/P-Erk pathway, which mimics FGF23 activity in DCT. (2) Proteolytic cleavage of membrane bound HBEGF is activated, then produces sHB which binds to EGFR/ErbB4 to stimulate the MAPK pathway. This is the hypothesized sHB function in the PT.

To verify whether this cell line was a proper model to test this hypothesized pathway, Western blots, immunofluorescence and q-PCR were used. Transfected mKL cells, either with empty vector DNA (PC-DNA) or HBEGF DNA, were treated with saline, FGF23 or Phorbol 12-myristate 13-acetate (TPA) for 15 minutes (Figure 12 a-c). This short time treatment was implemented because of the MAPK pathway's rapid signaling. TPA was added as a positive control for HBEGF cutting, which should increase cutting [58].

In q-PCR analysis (Figure 12a), vehicle transfected cells with FGF23 treatment showed a robust Egr1 mRNA induction compared to saline. This FGF23 activation marker proved that FGFR- α KL co-receptor worked for FGF23 binding as FGF23 treated empty plasmid transfected cells had increasing P-Erk expression (Figure 12b). For HBEGF transfected cells, Egr1 mRNA levels increased with ectopic FGF23 treatment. Whereas this increase was also observed in saline treated HBEGF transfected cells, which may be due to both uncut HBEGF and soluble HBEGF activating the MAPK pathway. Thus, unfortunately it could not be used as the evidence for supporting sHB, which might be formed through FGF23 triggered cutting through binding its receptor to activate the MAPK pathway. I next probed for EGFR signaling using Western blot. The P-EGFR band in PC-trans HBEGF treated cells confirmed that this cell model contained the correct receptor for HBEGF to elicit its downstream signals. The reason for a lack of signaling in HBEGF-trans cells lanes might be that after long-term exposure, 24 hours, HBEGF signaling was down regulated. Transfected cells were also stained by immunofluorescence with the laboratory made HBEGF antibody (Figure 12d). It was hypothesized that FGF23 and TPA treated HBEGF-transfected cells should have less staining compared with saline

treated cells due to the shedding of HBEGF. Unexpectedly, there was no noticeable difference between each group, even with different time point treatments (30-min, 6-hour, 24-hour, figures not shown).

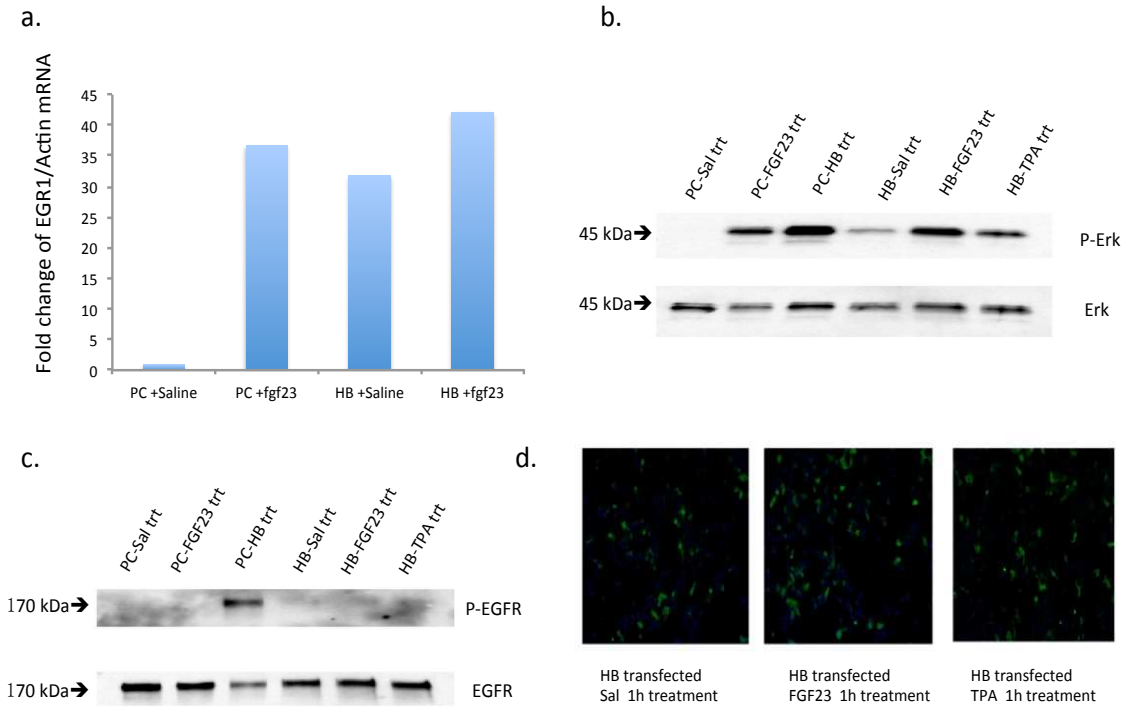


Figure 12 Potential cell model characterization

mKL cells (HEK293 cells) were transfected with either empty plasmid (PC DNA) or human HBEGF plasmid. (a) q-PCR analysis of cell RNA after treatment with saline or recombinant FGF23. (b), (c) Western blots of cell protein after treated with saline, FGF23, HBEGF or TPA, which were probed with anti-Erk, anti-P-Erk1/2, anti-EGFR, or anti-P-EGFR. (d) Immunostaining for differently treated cells (60 minutes treatment) with HBEGF antibody.

HBEGF signal mapping *in vivo*

In parallel experiments, mice were used to explore the localization of kidney HBEGF signaling *in vivo*. Four 12 week old WT mice were injected with vehicle (saline), 10 μ g FGF23 or 10 μ g HBEGF i.v., euthanized 10 minutes later, and tissues were collected. 8 μ m kidney sections were produced for immunofluorescence. Following laboratory staining protocols (see Material and Methods), each section was probed with anti-P-Erk1/2, anti-Klotho (KO603) or Fluorescein labeled Lotus Tetragonolobus Lectin (LTL), or co-probed with a combination of two reagents. LTL is a reliable PT marker that stains the brush border membrane, and mKL was used as a renal DCT marker.

q-PCR was run first to make sure the HBEGF injections were successful (Figure 13a). Each column represented each mouse's EGR1 gene change. Approximately 8-fold increases were seen in FGF23-injected mice and a more than 15-fold rise in the two HBEGF injected mice compared with vehicle treated mice (Figure 13a). After proving the treatments were delivered successfully into mice, immunostaining was performed to map HBEGF signaling.

Consistent with EGR1 expressional changes, HBEGF and FGF23 injected mice had more P-Erk1/2 staining than vehicle treated (Figure 13b). It was previously shown that FGF23 initiated Erk phosphorylation within ten minutes in the DCT [23]. As shown in Figure 14a, P-Erk1/2 and mKL were merged in yellow, indicating co-localization, and in Figure 14b, P-Erk1/2 did not overlap with LTL staining of the PT.

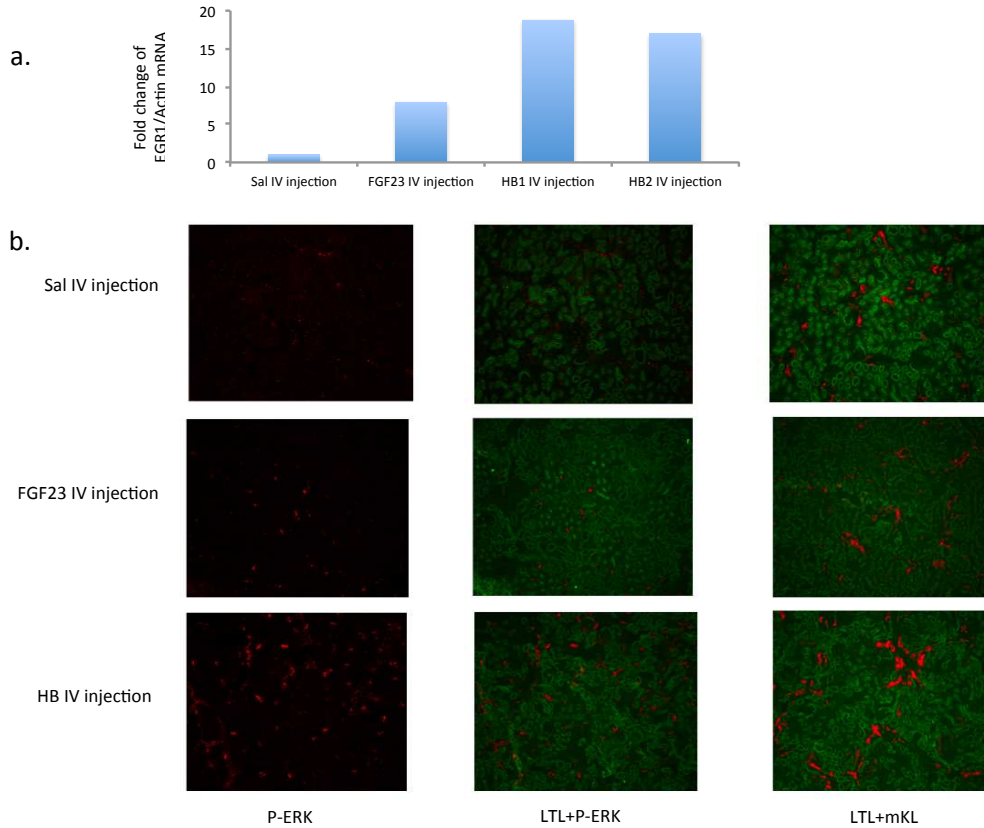


Figure 13 P-Erk staining mapping *in vivo* (1)

Mice received tail vein injections of vehicle, FGF23 or HBEGF (2 mice) and were sacrificed 10 min later. (a) Kidneys were collected and RNAs were extracted for EGR1 expression. (b) Kidneys were then collected for immunofluorescence. The first row was vehicle treated kidneys, second row was FGF23 treated and the third row was HBEGF treated. The first column was stained with P-ERK (red), the second column was co-stained for LTL (green) and P-ERK (red), and the third one was for LTL (green) and Klotho (red).

In the co-staining of P-Erk1/2 and LTL for HBEGF treated mice, the P-Erk staining seemed to be separated from LTL, which suggested the activation of MAPK pathway by HBEGF may occur in the renal DCT, similar to FGF23. If soluble HBEGF was the mediator to communicate between renal proximal tubule and DCT, then shortly after acute HB administration, P-Erk1/2 staining should have been evident in the PT. Unexpectedly, no overlapping of P-Erk1/2 and LTL was found in HBEGF injected mice, and partial mKL staining overlapped with P-Erk1/2 fluorescence.

Therefore, these studies suggest that HBEGF may signal in the renal DCT, not the renal PT. Taken together with the fact that HBEGF controls genes in the FGF23 pathway (shown above by qPCR in Figures 6 and 7), these results could indicate that HBEGF is downstream of FGF23 and elicits an important signal for FGF23 bioactivity *in vivo* in the DCT. However another factor may be downstream of HBEGF to act as a DCT-PT communicator (see revised model in Discussion).

In summary, studies showed that kidney HBEGF was induced by FGF23, and my work demonstrated that HBEGF has FGF23-like activity on key genes that control phosphate homeostasis *in vivo*. In addition, a specific HBEGF antibody was developed and characterized, and shown to recognize HBEGF protein by immunoblot and in cells. This novel tool will be useful for future experiments assessing HBEGF expression levels and activity. Finally, HBEGF signaling has never been mapped in the kidney *in vivo*. I have shown that HBEGF-mediated MAPK signaling localizes to the DCT more than the PT. Collectively, these studies support that HBEGF expression and activity is downstream of

FGF23. This thesis has now uncovered possible new roles for HBEGF in mediating DCT-specific FGF23 activity.

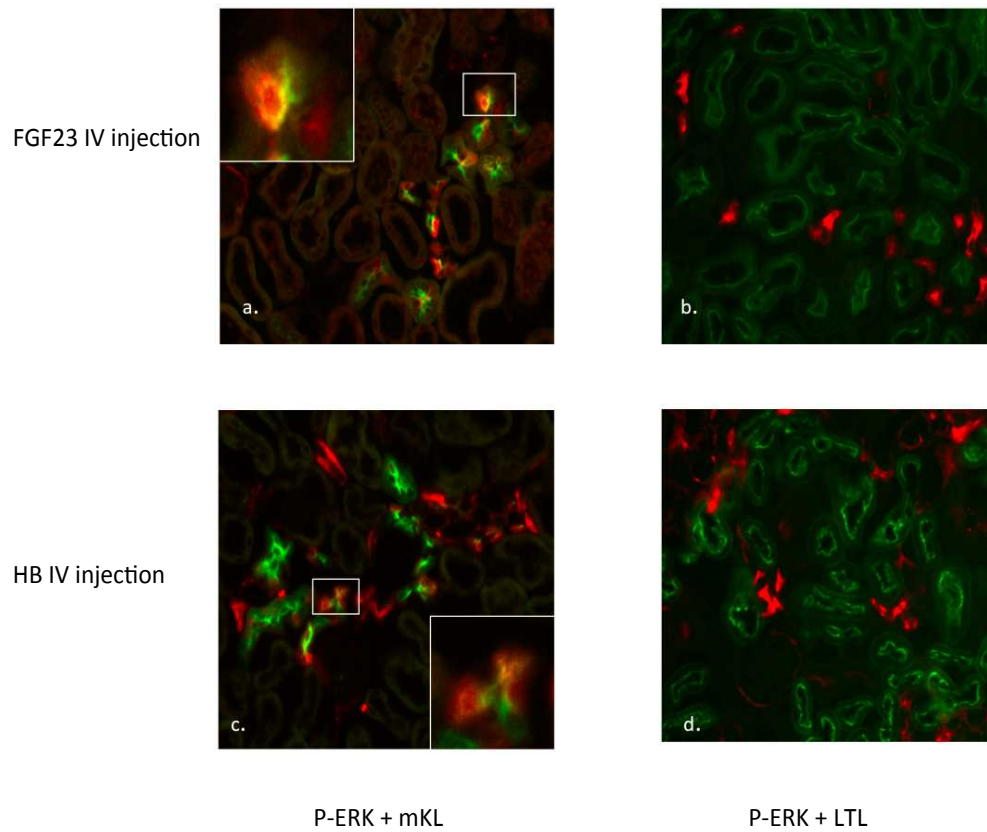


Figure 14 P-Erk staining mapping *in vivo* (2)

The first column (a and c) was co-stained for P-Erk1/2 (red) and mKL (green). The second column (b and d) was co-stained for P-Erk1/2 (red) and LTL (green). In FGF23 injected mice, P-Erk and mKL had some overlapping signals (a), whereas P-Erk did not stain the same region as LTL in PT (b). In HBEGF treated mice, P-Erk also partially overlapped with mKL staining (c), and P-Erk was separate from PT LTL fluorescence (d).

Discussion

Thesis summary

The signaling events underlying FGF23 bioactivity in the kidney are a major consideration for rare and common disorders that have disturbances in phosphate homeostasis. In CKD patients, the inability to remove excess phosphate drives FGF23 production, a known contributor to severe cardiovascular events and mortality [42]. Additionally, therapeutics such as FGF23 neutralization in these patients is not feasible since FGF23 still maintains some phosphaturic function. In agreement with this, previous rat CKD studies have found increased mortality when using an antibody against FGF23 [59]. Therefore, it is crucial to understand the signaling events that occur by FGF23 in the kidney to decrease both phosphate reabsorption and active vitamin D synthesis. Complicating the course of these studies is the fact that the co-receptor α KL resides on the renal DCT, whereas the downstream effects occur in the renal PT. This suggests a necessary communication between these two cell types to elicit NPT2a internalization and decreased 1α (OH)ase expression.

The mechanisms of how FGF23 signals trigger the spatially separate effects in kidney are currently unknown. Thus, microarray analysis was applied and was expected to illuminate additional downstream responses to FGF23 signaling. In the array analysis, HBEGF was found as the second-most increased mRNA, suggesting a correlation with FGF23 bioactivity in the kidney. In consideration of the molecular properties of HBEGF,

we hypothesized that cleaved and sHB may act as a paracrine factor traveling from the DCT to the PT, causing NPT2a protein down regulation and reducing the vitamin D $1\alpha(\text{OH})\text{ase}$. To test this hypothesis, both *in vivo* and *in vitro* experiments were performed.

This Discussion will describe other approaches to my studies that could be taken, as well as a possible alternative hypothesis due to my study outcomes.

***In vivo* study analysis**

Identifying involved gene changes in FGF23 signaling

At the outset of these studies, microarray analyses were utilized approximately eight years ago to test gene changes in the kidneys of mice administered FGF23. This approach produced the first indication for the role of HBEGF in the FGF23 signaling cascades. As new technologies have been more recently developed, RNA-seq has become a more powerful and comprehensive tool to study gene expression levels under various conditions. Compared to microarrays, next generation sequencing (NGS) has three main advantages: 1) No limitations to testing the existing genomic sequences (microarray can only quantify custom designed genes); 2) Larger dynamic range and lower background signals than microarray; 3) Higher accuracy and reproducibility [60]. Thus, with the decreasing cost of NGS, it would be feasible to repeat this mouse experiment using RNA-seq, which can provide us with potentially more information on expression level changes

with FGF23 treatment. It is possible that with this newer and more reliable technology, other genes could be identified to be more tightly involved in FGF23 signaling.

Gene expression changes in FGF23-related knockout mouse models

There exist two mouse models in which the FGF23 signaling is disrupted due to either the lack of hormone (FGF23-KO mice) or lack of the required FGF23 co-receptor (α KL-KO mice). Both models exhibit dramatic hyperphosphatemia and elevated $1\alpha(\text{OH})\text{ase}$ levels. To test the hypothesis of whether HBEGF signaling on the PT lies downstream of FGF23 signaling within the DCT, both mouse models were treated with sHB. As shown in Figure 6 and Figure 7, renal $1\alpha(\text{OH})\text{ase}$ expression levels decreased in both KL-KO and FGF23-KO mice with sHB administration compared to saline treated controls. These data supported our hypothesis that HBEGF is downstream of FGF23 activity, leading to the studies described below.

In the FGF23-KO mice injected with HBEGF and FGF23, there was a trend for decreasing $1\alpha(\text{OH})\text{ase}$ compared with vehicle treated FGF23-KO mice. However, these reductions were not statistically significant ($p > 0.05$). To improve this data, more FGF23-KO mice could be used in future studies. As the severity of the phenotype can be wide in these KO mouse models, increasing numbers of injected mice may be helpful to provide less variation for the analysis of gene expression.

In addition to optimizing our protocols further, novel mouse models could be generated to improve our studies and provide new ways to address our central hypothesis. For example, HB-KO mice and HB overexpressed transgenic mice, could potentially provide more straightforward information for HBEGF function in the kidney. In previous studies, HBEGF global KO mice were generated. Due to HBEGF's wide tissue distribution and central role in multiple biological activities, the global HB-KO mice have very short life span and severe systemic defects [57]. In order to better study HBEGF function in the kidney, conditional HBEGF KO mice could be generated using the Cre-Lox recombination system. The IU transgenic Core could produce floxed HBEGF mice, which have lox-p sites flanking critical exons in the HBEGF gene. These Flox HBEGF mice would then be cross bred with Ksp-Cre transgenic mice to derive conditional HBEGF KO mice with no HBEGF expression in renal tubular cells. The Ksp-Cre recombinase is driven by the 1.3kb promoter of mouse Ksp-cadherin which is expressed exclusively in renal tubular epithelial cells [61]. We expect the Ksp-driven HBEGF conditional KO mice would present with hyperphosphatemia and increased $1\alpha(\text{OH})\text{ase}$ levels, mimicking FGF23-KO and KL-KO mouse models. Additionally, conditional HBEGF knock-in transgenic mice can also be generated, with HBEGF overexpression in the kidney using Ksp-Cre. If HBEGF functions as hypothesized above, this knock-in mouse model would likely show hypophosphatemia, decreased $1\alpha(\text{OH})\text{ase}$ expression and related symptoms, which are opposite to the HBEGF KO mouse model. Conditional HBEGF knock-in mice would have a long-term HBEGF expression instead of short-term injections as performed in my studies, potentially providing new insight into HBEGF renal actions.

HBEGF pathway immunofluorescence in kidney sections

It has been shown in previous studies that membrane bound HBEGF is primarily produced in the kidney DCT [47]. We hypothesized HBEGF would be cleaved in the renal DCT upon FGF23 signaling and travel to the renal PT to initiate downstream signals, functioning through the MAPK pathway. Previous studies have found the major transcription factor to regulate the gene expression changes upon FGF23 stimulation is Egr1, which is activated through the MAPK signaling [62]. Importantly, with sHB injection I found a significant increase in renal Egr1 expression, demonstrating upstream activation of the MAPK pathway.

Immunofluorescence is a powerful tool to determine locations of proteins. In this regard, treated kidneys were sectioned and stained for P-Erk to determine the spatial location of its activation. These studies, in concordance with previous data, showed P-Erk staining increased with FGF23 treatment and overlapped with α KL staining in the renal DCT (Figure 14a). However, in HBEGF injected mice, P-Erk and α KL signals partially overlapped in the renal DCT and the P-Erk and LTL staining was separated, indicating that HBEGF administration seemed to function on the renal DCT, in contrast to our original hypothesis that HBEGF worked directly on the renal PT.

In these immunofluorescence experiments, further analyses could be undertaken. These include using additional antibodies recognizing specific signaling molecules to test HBEGF bioactivity in the kidney. For example, antibodies recognizing

EGFR/ErbB1/HER1 and ErbB4/HER4, receptors for HBEGF could be tested. In these experiments, WT mice could be given i.v. injections with FGF23, HBEGF or TPA, and sacrificed 10-min, 30-min or 60-min afterwards. Since the specific time courses for HBEGF signaling is not clear, different time points should be tested. Then anti-phospho-EGFR and anti-phospho-HER4 antibodies could be applied by staining to provide us with additional localization of HBEGF receptor localization.

***In vitro* study analysis**

A cell model being tested

Due to the small size of sHB, an *in vitro* model was developed to study the FGF23 initiated cleavage of membrane bound HBEGF. In this regard, HEK293 cells already stably transfected with membrane bound KL (α KL) were utilized as they had been previously shown to elicit the MAPK signaling with FGF23 stimulation [23]. To test our hypothesis, a plasmid expressing mouse membrane bound HBEGF was transfected into the cells to ensure that the cells containing essential molecules for FGF23 signaling studies.

Interestingly, the results showed an increase in Egr1 expression, a known target of P-Erk1/2, in HBEGF transfected mKL cells without FGF23 treatment. This increase lasted for more than 48 hours. Unfortunately, we found no further Egr1 induction when the transfected cells were treated with FGF23. With this continual stimulation, this action

may deplete cellular signals and cause resistance to FGF23 function. Due to the fact that both FGF23 and HBEGF stimulated the MAPK pathway, unfortunately we could not delineate the activation of the individual proteins in these cells. Additionally, HBEGF immunofluorescence of saline, FGF23 or TPA treated cells showed no HBEGF protein differences on the cell membrane (Figure 12d), suggesting: 1) HBEGF was not being cleaved by signaling events initiated from exogenous proteins in this cell model, therefore an alternative cell model may be required to study these signaling events; and, 2) HBEGF production from the plasmid was so highly elevated that cutting did not lead to detectable changes when treated with FGF23 or TPA.

In vitro study optimization

There are several approaches that could be taken to optimize these studies. In this regard, a Tet-on inducible system could be used to control HBEGF expression in cells. The mKL cell line would be transfected with two major components for Tet-on system, the regulator plasmid and the response plasmid. The regulator plasmid produces rtTA (reverse tetracycline-controlled transactivator), while the response plasmid contains a TRE sequence upstream of the HBEGF gene in our study. Once the rtTA binds to TRE (tetracycline-response element) in the presence of Dox (doxycycline), HBEGF would be expressed [63]. More importantly, the induction can be tested within an optimized time frame and with different Dox exposure concentrations to adjust HBEGF protein levels carefully. After determining the optimal induction time, treatments could be applied. This

tightly regulated new cell line could be helpful to study FGF23-HBEGF signaling events without continuously and highly expressed HBEGF.

Further, to get an explicit understanding of FGF23 signaling effects on HBEGF, an EGFR “knock-out” cell model (perhaps in HEK293 cells) could also be generated using CRISPR (clustered regularly interspaced short palindromic repeat)/Cas (CRISPR-associate endonuclease) 9 system. A guide RNA could be designed first to bind with Cas9 and lead the endonuclease to cleave the cell’s EGFR gene at the specific site within the coding region. The resulting double strand breaks would be repaired by an error-prone non-homologous end joining (NHEJ) pathway, resulting in small insertions or deletions at the break site and disrupting EGFR expression[64]. Cell clones with successful deletion would be chosen and cultured. With EGFR deletion, transfected HBEGF protein cannot elicit the MAPK pathway signaling, so that Egr1 could potentially be used as a marker for FGF23 signaling in this cell model. Additionally, cell media could be collected for sHB protein testing in response to FGF23 administration downstream of KL signaling.

Finally, different cell models can be tested as well. For example, monkey kidney Vero cells overexpressing HBEGF (Vero-H) were previously used to study the relationship between reactive oxygen species (ROS) and HBEGF shedding [58]. In this study, HBEGF shedding in Vero-H cells was observed using immunoblots, which detected the full-length form and the cytoplasmic fragment. Vero-H cells do not express α KL, thus, to utilize this cell line, stable transfection of α KL would need to be performed first. After

isolating this cell line, the cells could be treated with FGF23 and collected, then the anti-HBEGF antibody I characterized could be used to test whether the cleavage is FGF23-dependent.

Alternative hypothesis to FGF23 signaling

With regard to another possible DCT-PT factor, previous studies have suggested that α KL might be the mediator of DCT and PT communication. On the one hand, KL has been weakly detected in the renal PT using immunofluorescence and Western blots [65], consistent with direct signaling of KL in the PT to mediate FGF23 activity. On the other hand, another possibility is that α KL is also cleaved to a soluble form, acting as a paracrine factor from DCT to PT. In support of this model, others have described a serum phosphate reduction due to decreased NPT2a reabsorption in transgenic mice overexpressing KL [65]. However, in our study, strong α KL signals were exclusively observed in the renal DCT without any α KL staining in the PT (see Figure 15). As the marker LTL specifically stained renal PT, and α KL signals were clearly separated from LTL, this strongly suggested α KL expressed in the renal DCT but not the proximal tubules. Due to the fact that upon FGF23 injection, P-Erk1/2 staining only appears to co-localize with α KL staining and is exclusive to DCT, we do not believe there is any α KL in the PT to contribute to FGF23 signaling events.

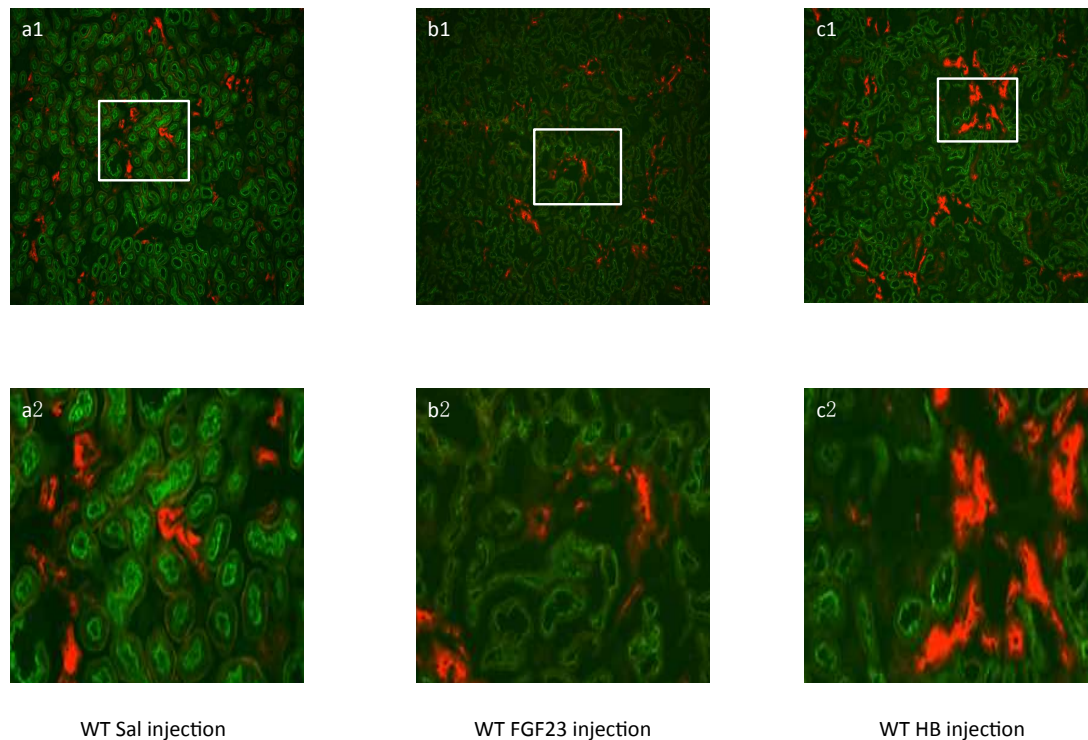


Figure 15 α KL mapping in the kidneys

In initial studies, WT mice were i.v. injected with either saline or FGF23 or HBEGF.

Kidney sections were co-stained with anti- α KL antibody (red) and LTL (green). a2, b2 and c2 were enlarged images of a1, b1 and c1's chosen areas in frames. No overlapping staining was observed.

In my initial studies undertaken by q-PCR analysis, FGF23-KO and KL-KO mice were observed as having highly increased $1\alpha(\text{OH})\text{ase}$ levels due to the lack of FGF23 bioactivity. Delivery of HBEGF largely corrected this increases, demonstrating its importance in controlling phosphate handling genes. In my subsequent studies, HBEGF cleavage *in vitro* did not appear to be FGF23-dependent. Additionally, HBEGF activation of the MAPK pathway occurred in the DCT and did not appear to affect NPT2 protein *in vivo*. Thus, HBEGF may be only a portion of the downstream signaling for the FGF23 pathway. Further, HBEGF may therefore be required to elicit another mediator to communicate between the renal DCT and PT. Therefore, an alternative hypothesized pathway can be proposed (see Figure 16) where FGF23 activated KL in the renal DCT, which then signals through HBEGF, also on the DCT, eliciting a factor that is responsible for PT-localized FGF23 bioactivity.

Conclusion

In conclusion, we have found a novel role for HBEGF as a downstream mediator of the FGF23 signaling pathways in the kidney. This opens up new avenues to better understand renal phosphate handling, in addition to possible development of novel therapeutics. While injection of sHB demonstrated similar activities to FGF23 with decreased $1\alpha(\text{OH})\text{ase}$ expression, it remains unclear whether the initiation of membrane bound HBEGF cleavage is FGF23 dependent. Additionally, immunofluorescent staining has yet to illustrate P-Erk1/2 signaling within the proximal tubule cells upon either FGF23 or HBEGF injections. Therefore, further studies in the optimized cell culture and

conditional mouse models as proposed above will aid in understanding the steps of the FGF23 signaling cascade for phosphate homeostasis.

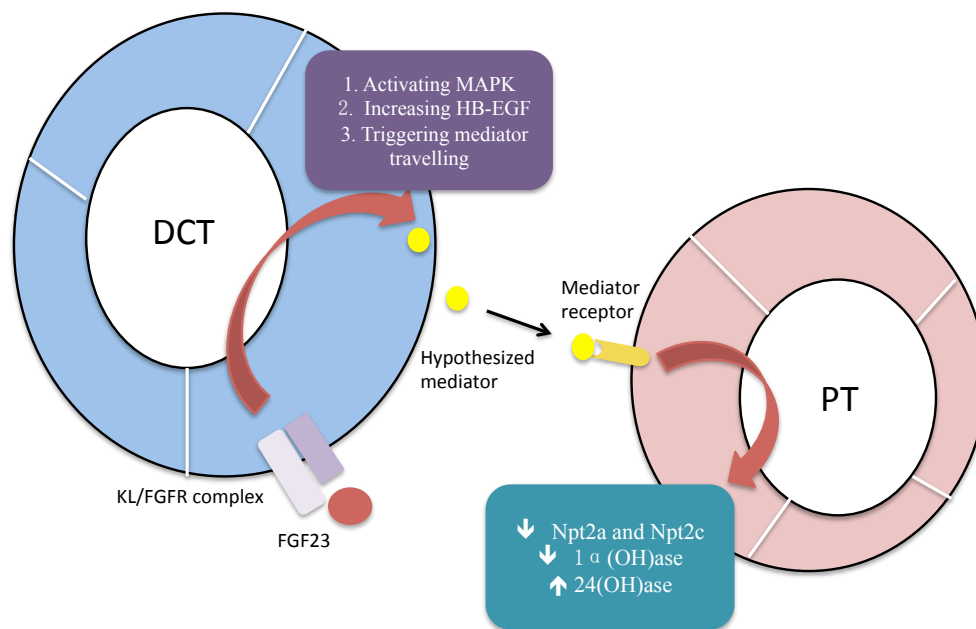


Figure 16 Alternative hypothesized pathway for renal FGF23 signaling

Within the DCT, FGF23 could bind to the KL/FGFR complex to activate downstream signals. Activation of the MAPK pathway increase HBEGF expression levels as well as an unknown DCT-PT mediator. This unknown mediator transmits FGF23 signals from the renal DCT to the PT, leading to phosphate regulation downstream of FGF23 and HBEGF.

References

1. Wang, M., J.D. Hanna, and J.C.M. Chan, *Phosphate Nutrition*, in *Phosphate in Pediatric Health and Disease*, U. Alon and J.C.M. Chan, Editors. 1993.
2. Wasserman, R.H. and A.N. Taylor, *Intestinal absorption of phosphate in the chick: effect of vitamin D and other parameters*. J Nutr, 1973. **103**(4): p. 586-99.
3. White, K.E., F.R. Bringhurst, and M.J. Econs, *Genetic Disorders of Phosphate Homeostasis*, in *Endocrinology Adult and Pediatric: The Parathyroid Gland and Bone Metabolism*, J. John T. Potts, J.L. Jameson, and L.J.D. Groot, Editors. 2010.
4. Beck, L., et al., *Targeted inactivation of Npt2 in mice leads to severe renal phosphate wasting, hypercalciuria, and skeletal abnormalities*. Proc Natl Acad Sci U S A, 1998. **95**(9): p. 5372-7.
5. Shimada, T., et al., *Cloning and characterization of FGF23 as a causative factor of tumor-induced osteomalacia*. Proc Natl Acad Sci U S A, 2001. **98**(11): p. 6500-5.
6. Pfister, M.F., et al., *Parathyroid hormone-dependent degradation of type II Na⁺/Pi cotransporters*. J Biol Chem, 1997. **272**(32): p. 20125-30.
7. Juppner, H., et al., *A G protein-linked receptor for parathyroid hormone and parathyroid hormone-related peptide*. Science, 1991. **254**(5034): p. 1024-6.
8. Gardella, T.J., et al., *Parathyroid Hormone and Parathyroid Hormone-Related Peptide in the Regulation of Calcium Homeostasis and Bone Development*, in *Endocrinology Adult and Pediatric: The Parathyroid Gland and Bone Metabolism*, J. John T. Potts, J.L. Jameson, and L.J.D. Groot, Editors. 2010.
9. Itoh, N. and D.M. Ornitz, *Evolution of the Fgf and Fgfr gene families*. Trends Genet, 2004. **20**(11): p. 563-9.
10. *Autosomal dominant hypophosphataemic rickets is associated with mutations in FGF23*. Nat Genet, 2000. **26**(3): p. 345-8.
11. Shimada, T., et al., *Mutant FGF-23 responsible for autosomal dominant hypophosphatemic rickets is resistant to proteolytic cleavage and causes hypophosphatemia in vivo*. Endocrinology, 2002. **143**(8): p. 3179-82.
12. Rimmucci, M., et al., *FGF-23 in fibrous dysplasia of bone and its relationship to renal phosphate wasting*. J Clin Invest, 2003. **112**(5): p. 683-92.
13. Shimada, T., et al., *FGF-23 is a potent regulator of vitamin D metabolism and phosphate homeostasis*. J Bone Miner Res, 2004. **19**(3): p. 429-35.
14. Larsson, T., et al., *Transgenic mice expressing fibroblast growth factor 23 under the control of the alpha1(I) collagen promoter exhibit growth retardation, osteomalacia, and disturbed phosphate homeostasis*. Endocrinology, 2004. **145**(7): p. 3087-94.
15. Aono, Y., et al., *Anti-FGF-23 neutralizing antibodies ameliorate muscle weakness and decreased spontaneous movement of Hyp mice*. J Bone Miner Res, 2011. **26**(4): p. 803-10.
16. Perwad, F., et al., *Dietary and serum phosphorus regulate fibroblast growth factor 23 expression and 1,25-dihydroxyvitamin D metabolism in mice*. Endocrinology, 2005. **146**(12): p. 5358-64.
17. Burnett, S.M., et al., *Regulation of C-terminal and intact FGF-23 by dietary phosphate in men and women*. J Bone Miner Res, 2006. **21**(8): p. 1187-96.

18. Ornitz, D.M. and N. Itoh, *Fibroblast growth factors*. Genome Biol, 2001. **2**(3): p. Reviews3005.
19. Zhang, X., et al., *Receptor specificity of the fibroblast growth factor family. The complete mammalian FGF family*. J Biol Chem, 2006. **281**(23): p. 15694-700.
20. Kurosu, H., et al., *Regulation of fibroblast growth factor-23 signaling by klotho*. J Biol Chem, 2006. **281**(10): p. 6120-3.
21. Matsumura, Y., et al., *Identification of the human klotho gene and its two transcripts encoding membrane and secreted klotho protein*. Biochem Biophys Res Commun, 1998. **242**(3): p. 626-30.
22. Imura, A., et al., *Secreted Klotho protein in sera and CSF: implication for post-translational cleavage in release of Klotho protein from cell membrane*. FEBS Lett, 2004. **565**(1-3): p. 143-7.
23. Farrow, E.G., et al., *Initial FGF23-mediated signaling occurs in the distal convoluted tubule*. J Am Soc Nephrol, 2009. **20**(5): p. 955-60.
24. Clinkenbeard, E.L., *A Murine Model with Conditional FGF23 Deletion*. Journal of Bone and Mineral Research, 2015.
25. Kuro-o, M., et al., *Mutation of the mouse klotho gene leads to a syndrome resembling ageing*. Nature, 1997. **390**(6655): p. 45-51.
26. Econs, M.J. and P.T. McEnery, *Autosomal dominant hypophosphatemic rickets/osteomalacia: clinical characterization of a novel renal phosphate-wasting disorder*. J Clin Endocrinol Metab, 1997. **82**(2): p. 674-81.
27. Imel, E.A., S.L. Hui, and M.J. Econs, *FGF23 concentrations vary with disease status in autosomal dominant hypophosphatemic rickets*. J Bone Miner Res, 2007. **22**(4): p. 520-6.
28. Durham, B.H., et al., *The association of circulating ferritin with serum concentrations of fibroblast growth factor-23 measured by three commercial assays*. Ann Clin Biochem, 2007. **44**(Pt 5): p. 463-6.
29. Ruppe, M.D., *X-Linked Hypophosphatemia*, in *GeneReviews(R)*, R.A. Pagon, et al., Editors. 1993, University of Washington, Seattle
University of Washington, Seattle. All rights reserved.: Seattle (WA).
30. *A gene (PEX) with homologies to endopeptidases is mutated in patients with X-linked hypophosphatemic rickets. The HYP Consortium*. Nat Genet, 1995. **11**(2): p. 130-6.
31. Yamazaki, Y., et al., *Increased circulatory level of biologically active full-length FGF-23 in patients with hypophosphatemic rickets/osteomalacia*. J Clin Endocrinol Metab, 2002. **87**(11): p. 4957-60.
32. Liu, S., et al., *Regulation of fibroblastic growth factor 23 expression but not degradation by PHEX*. J Biol Chem, 2003. **278**(39): p. 37419-26.
33. Beck, L., et al., *Pex/PEX tissue distribution and evidence for a deletion in the 3' region of the Pex gene in X-linked hypophosphatemic mice*. J Clin Invest, 1997. **99**(6): p. 1200-9.
34. Feng, J.Q., et al., *Loss of DMP1 causes rickets and osteomalacia and identifies a role for osteocytes in mineral metabolism*. Nat Genet, 2006. **38**(11): p. 1310-5.
35. Levy-Litan, V., et al., *Autosomal-recessive hypophosphatemic rickets is associated with an inactivation mutation in the ENPP1 gene*. Am J Hum Genet, 2010. **86**(2): p. 273-8.

36. Nam, H.K., et al., *Ectonucleotide pyrophosphatase/phosphodiesterase-1 (ENPP1) protein regulates osteoblast differentiation*. J Biol Chem, 2011. **286**(45): p. 39059-71.
37. Mitnick, P.D., et al., *Calcium and phosphate metabolism in tumoral calcinosis*. Ann Intern Med, 1980. **92**(4): p. 482-7.
38. Garringer, H.J., et al., *The role of mutant UDP-N-acetyl-alpha-D-galactosamine-polypeptide N-acetylgalactosaminyltransferase 3 in regulating serum intact fibroblast growth factor 23 and matrix extracellular phosphoglycoprotein in heritable tumoral calcinosis*. J Clin Endocrinol Metab, 2006. **91**(10): p. 4037-42.
39. Frishberg, Y., et al., *Hyperostosis-hyperphosphatemia syndrome: a congenital disorder of O-glycosylation associated with augmented processing of fibroblast growth factor 23*. J Bone Miner Res, 2007. **22**(2): p. 235-42.
40. Coresh, J., et al., *Prevalence of chronic kidney disease in the United States*. Jama, 2007. **298**(17): p. 2038-47.
41. *Kidney Disease: Improving Global Outcomes (KDIGO) CKD-MBD Work Group, in KDIGO clinical practice guideline for the diagnosis, evaluation, prevention, and treatment of Chronic Kidney Disease-Mineral and Bone Disorder (CKD-MBD)*. 2009.
42. Fliser, D., et al., *Fibroblast growth factor 23 (FGF23) predicts progression of chronic kidney disease: the Mild to Moderate Kidney Disease (MMKD) Study*. J Am Soc Nephrol, 2007. **18**(9): p. 2600-8.
43. Gutierrez, O.M., et al., *Fibroblast growth factor 23 and mortality among patients undergoing hemodialysis*. N Engl J Med, 2008. **359**(6): p. 584-92.
44. Farrow, E.G., et al., *Altered renal FGF23-mediated activity involving MAPK and Wnt: effects of the Hyp mutation*. J Endocrinol, 2010. **207**(1): p. 67-75.
45. Fukuda, T., et al., *FGF23 induces expression of two isoforms of NAB2, which are corepressors of Egr-1*. Biochem Biophys Res Commun, 2007. **353**(1): p. 147-51.
46. Lin, B.C., et al., *Liver-specific activities of FGF19 require Klotho beta*. J Biol Chem, 2007. **282**(37): p. 27277-84.
47. Higashiyama, S., et al., *Structure of heparin-binding EGF-like growth factor. Multiple forms, primary structure, and glycosylation of the mature protein*. J Biol Chem, 1992. **267**(9): p. 6205-12.
48. Groenestege, W.M., et al., *Impaired basolateral sorting of pro-EGF causes isolated recessive renal hypomagnesemia*. J Clin Invest, 2007. **117**(8): p. 2260-7.
49. Besner, G., S. Higashiyama, and M. Klagsbrun, *Isolation and characterization of a macrophage-derived heparin-binding growth factor*. Cell Regul, 1990. **1**(11): p. 811-9.
50. Higashiyama, S., et al., *A heparin-binding growth factor secreted by macrophage-like cells that is related to EGF*. Science, 1991. **251**(4996): p. 936-9.
51. Vinante, F. and A. Rigo, *Heparin-binding epidermal growth factor-like growth factor/diphtheria toxin receptor in normal and neoplastic hematopoiesis*. Toxins (Basel), 2013. **5**(6): p. 1180-1201.
52. Thompson, S.A., et al., *Characterization of sequences within heparin-binding EGF-like growth factor that mediate interaction with heparin*. J Biol Chem, 1994. **269**(4): p. 2541-9.

53. Nanba, D., et al., *Proteolytic release of the carboxy-terminal fragment of proHB-EGF causes nuclear export of PLZF*. J Cell Biol, 2003. **163**(3): p. 489-502.
54. Raab, G. and M. Klagsbrun, *Heparin-binding EGF-like growth factor*. Biochim Biophys Acta, 1997. **1333**(3): p. F179-99.
55. Wajant, H., M. Grell, and P. Scheurich, *TNF receptor associated factors in cytokine signaling*. Cytokine Growth Factor Rev, 1999. **10**(1): p. 15-26.
56. Le Gall, S.M., et al., *ADAMs 10 and 17 represent differentially regulated components of a general shedding machinery for membrane proteins such as transforming growth factor alpha, L-selectin, and tumor necrosis factor alpha*. Mol Biol Cell, 2009. **20**(6): p. 1785-94.
57. Jackson, L.F., et al., *Defective valvulogenesis in HB-EGF and TACE-null mice is associated with aberrant BMP signaling*. Embo j, 2003. **22**(11): p. 2704-16.
58. Umata, T., *Involvement of reactive oxygen species in stimuli-induced shedding of heparin-binding epidermal growth factor-like growth factor*. J uoeh, 2014. **36**(2): p. 105-14.
59. Shalhoub, V., et al., *FGF23 neutralization improves chronic kidney disease-associated hyperparathyroidism yet increases mortality*. J Clin Invest, 2012. **122**(7): p. 2543-53.
60. Wang, Z., M. Gerstein, and M. Snyder, *RNA-Seq: a revolutionary tool for transcriptomics*. Nat Rev Genet, 2009. **10**(1): p. 57-63.
61. Shao, X., et al., *A minimal Ksp-cadherin promoter linked to a green fluorescent protein reporter gene exhibits tissue-specific expression in the developing kidney and genitourinary tract*. J Am Soc Nephrol, 2002. **13**(7): p. 1824-36.
62. Guha, M., et al., *Lipopolysaccharide activation of the MEK-ERK1/2 pathway in human monocytic cells mediates tissue factor and tumor necrosis factor alpha expression by inducing Elk-1 phosphorylation and Egr-1 expression*. Blood, 2001. **98**(5): p. 1429-39.
63. Gossen, M., et al., *Transcriptional activation by tetracyclines in mammalian cells*. Science, 1995. **268**(5218): p. 1766-9.
64. Mali, P., et al., *RNA-guided human genome engineering via Cas9*. Science, 2013. **339**(6121): p. 823-6.
65. Hu, M.C., et al., *Klotho: a novel phosphaturic substance acting as an autocrine enzyme in the renal proximal tubule*. Faseb j, 2010. **24**(9): p. 3438-50.

CURRICULUM VITAE

PU NI

Education

MS, Medical and Molecular Genetics

Indiana University, Indianapolis, IN. September 2013–December 2015

GPA: 3.95/4.0

Thesis: Testing the renal signaling axis for FGF23

Bachelor of Medicine

Anhui Medical University, The First Clinical College, China. September 2007–June 2012

GPA: 3.5/4.0

Outstanding Graduate Certificate

Experience

Research Assistant

Department of Medical and Molecular Genetics, IU April 2014 – December 2015

- Investigated phosphate homeostasis pathways in kidney on mouse models and mammalian cell lines, by performing molecular biology techniques, for example, RNA/protein extraction, Western Blot, RT-PCR, immunofluorescent staining, ELISA, etc.

- Conducted mouse handling, colony management, tissue collecting, IP injection.
- Analyzed data for statistical purposes.

Part Time Laboratory Assistant

Department of Medical and Molecular Genetics, IU June 2014 – December 2015

- Conducted DNA extraction and analysis (PCR) from tissue collected from specific mouse strains to provide information for mouse colony management needs in the laboratory.
- Helped with laboratory maintenance, including ordering, making stock solutions, etc.

Undergraduate Innovation Experiment

Anhui Medical University, China September 2010 – December 2010

- Worked in a student team to study the effects of an ApoE gene knockout on the expression of amyloid protein β in mice and investigated its possible relation with Alzheimer Disease's pathogenesis.

Publications

- Ning Zhang, Pu Ni, Lingfan Xu, et al. The expression change of amyloid protein β in the hippocampal neurons of ApoE knock out mice. *Acta University Medicinalis Anhui, Vol 46, 2011.*

- Erica L. Clinkenbeard, Taryn A. Cass, Pu Ni, Julia M. Hum, Teresita Bellido, Matthew R. Allen, and Kenneth E. White. Conditional Deletion of Murine FGF23: Interruption of Phosphate Sensing in Bone and Genetic Hypophosphatemia Rescue. 2015. *Pending submission.*

Volunteer Work

Laboratory Assistant for Tissue Culture Event January 2014, November 2014

Indiana University Simon Cancer Center, Indianapolis, IN

International Graduate Welcome Volunteer June 2015 – December 2015

Indiana University Simon Cancer Center, Indianapolis, IN